Chapter 11

The African turquoise killifish (*Nothobranchius furzeri*): biology and research applications

Gwendoline Astre*, **Eitan Moses***, **Itamar Harel**
Department of Genetics, The Silberman Institute, The Hebrew University of Jerusalem, Jerusalem, Israel

Introduction

There are more than 1200 killifish species, which populate almost every continent aside from Australia and Antarctica. Most killifish are small fish with an average size of 2.5−7 cm, and can be roughly divided into short-lived annual species and longer-lived nonannuals. Killifish are members of the Cyprinodontiform order, also known as "toothcarps," an order of ray-finned fish that includes several families (such as Aplocheilidae, Nothobranchiidae, Cyprinodontidae, Fundulidae, and others) (Nelson et al., 2016; Scheel, 1990). In recent years, the annual African turquoise killifish (*Nothobranchius furzeri*) has emerged as an exciting model system for experimental vertebrate aging due to its naturally compressed lifespan, rapid sexual maturity, embryonic diapause (a mechanism for survival during the dry season), and short generation time (Cellerino et al., 2015; Harel and Brunet, 2015; Kim et al., 2016; Platzer and Englert, 2016) (Fig. 11.1). These life history traits are probably an adaptation to its seasonal habitat, ephemeral water pans in southeast Africa, primarily Zimbabwe and Mozambique, where water is available only during the brief rainy season (Cellerino et al., 2015; Harel and Brunet, 2015; Kim et al., 2016; Platzer and Englert, 2016) (Fig. 11.2A). The turquoise killifish was first collected in 1968 in the Gonarezhou National Park (Zimbabwe). The inbred GRZ strain, named after the name of the park **G**ona**R**e**Z**hou (which means "Place of Elephants" in the local Shona dialect) is presently the most

* Equal contribution.

Laboratory Fish in Biomedical Research. https://doi.org/10.1016/B978-0-12-821099-4.00011-0

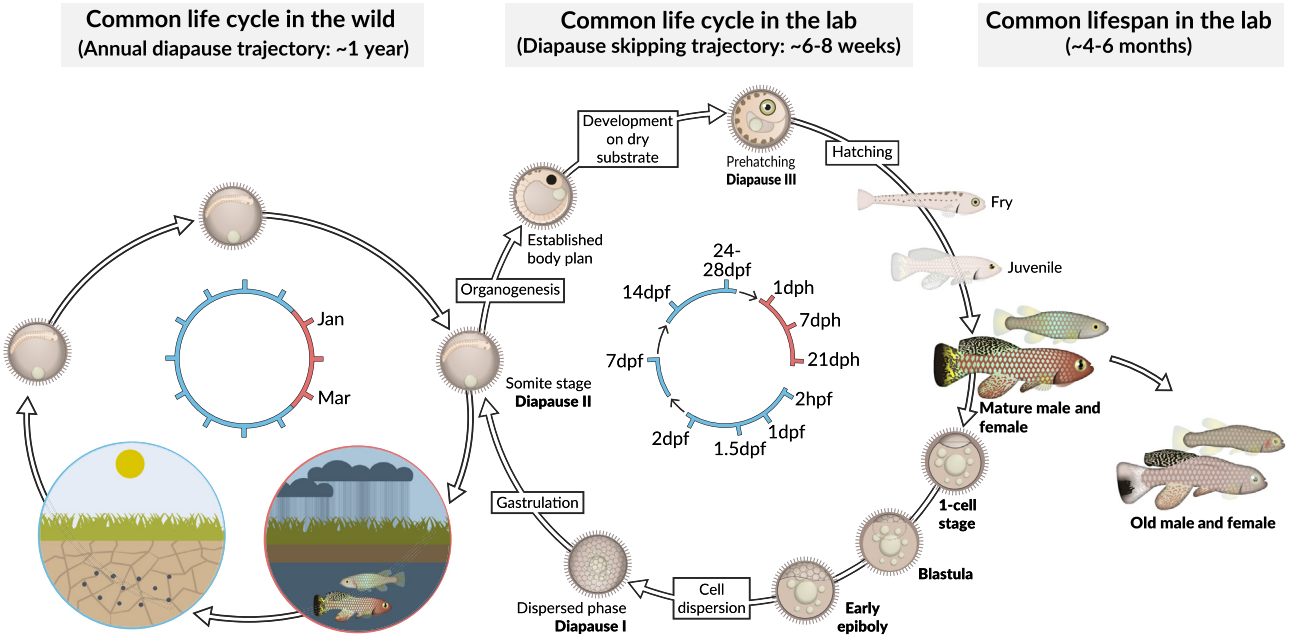

FIGURE 11.1 The life cycle of the turquoise killifish *Nothobranchius furzeri*, including the two common developmental trajectories. *Left*: In the wild, during the brief rainy season, the eggs from the previous year hatch and the fry rapidly reach sexual maturity, mate, and lay a new batch of eggs. These eggs will then enter a developmental arrest state called diapause, which commonly lasts for several months and protects the embryos during the dry season. Less common developmental trajectories, such as "diapause skipping" in the wild, or diapause that lasts for several years, are also possible and described elsewhere (Cellerino et al., 2015). *Center*: In the lab, the "diapause skipping" trajectory is largely preferred for practical reasons, and its primary stages and accompanying timeline are described. Although diapause can occur in three separate stages (diapause I, II, and III), the most common state is diapause II. A bias toward the "diapause skipping" trajectory can be achieved in the lab by controlling incubation temperatures (see the "Breeding strategies for genome engineering, including egg collection and incubation" section). Note that diapause I (dispersed phase) uncouples epiboly from gastrulation. *Right*: After approximately 3 weeks, fish reach sexual maturity. Male fish are larger and more colorful than the females. After a few months, old fish can display various signs of aging, including loss of muscle mass (i.e., sarcopenia) accompanied by bending of the spine (i.e., kyphosis), a global loss of pigmentation (or aberrant pigmentation patterns, as seen here in the tail), delayed wound healing (as seen here in the gills of the female), opaque lens, etc. *dpf*, days postfertilization.

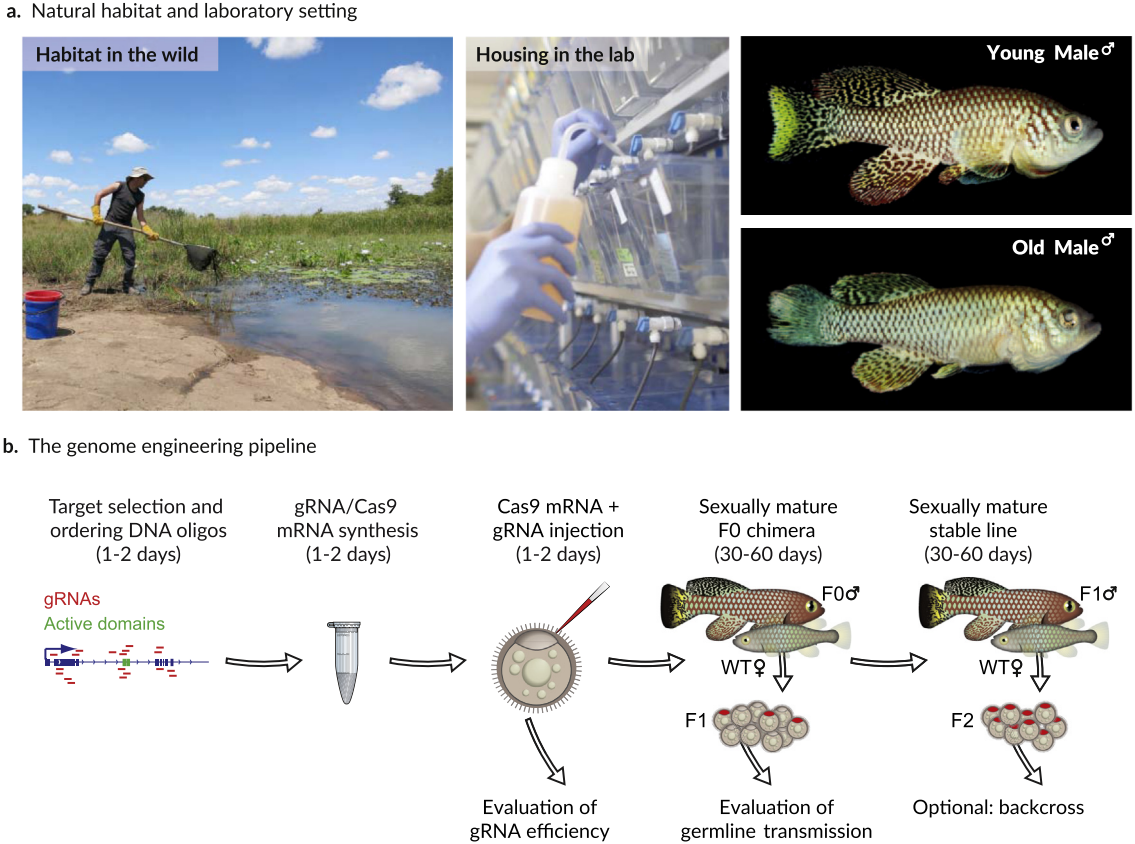

FIGURE 11.2 (A) The natural habitat of the turquoise killifish are ephemeral pans in Zimbabwe and Mozambique (*left*). In the lab, fish are housed in water recirculating systems (*middle*). An example of a young and an old male turquoise killifish (*right*). Although old fish can display various signs of aging, fish usually display only a subset. Here, loss of muscle mass (i.e., sarcopenia), a global loss of pigmentation, and an opaque lens are visible. (B) An efficient and rapid genome engineering pipeline for generating stable mutant fish lines in the turquoise killifish, including a detailed timeline. *gRNA*, guide RNA; *WT*, wild type. *Photo credits: Itamar Harel. Panel (B) is adapted with permission from Harel, I., Valenzano, D.R., Brunet, A., 2016. Efficient genome engineering approaches for the short-lived African turquoise killifish. Nat. Protoc.*

widely used laboratory strain. In this chapter we describe up-to-date husbandry guidelines to establish a large-scale killifish colony. We further provide detailed protocols for efficient genome engineering approaches (i.e. CRISPR/Cas9 and Tol2 strategies), which include reagent selection and synthesis, microinjection, genotyping, and troubleshooting.

As the most diverse group of vertebrates, fish species display extreme differences in the rate of life history traits, including lifespan. Interestingly, maximal lifespan between species is manifested as a continuum on a logarithmic scale, with more than a 1000-fold difference between extremes. On the one hand, the rockfish and the Greenland shark can live for several centuries (Nielsen et al., 2016; Tacutu et al., 2018), and on the other hand, the turquoise killifish and pygmy goby live for only several months (Cellerino et al., 2015; Depczynski and Bellwood, 2005; Harel and Brunet, 2015; Kim et al., 2016; Platzer and Englert, 2016). Aging has been studied in several fish species, either in comparative or experimental models, including salmon (Carney Almroth et al., 2012; Maldonado et al., 2000, 2002), zebrafish (Almaida-Pagan et al., 2014; Anchelin et al., 2013; Cardona-Costa et al., 2009; Gilbert et al., 2014b; Henriques et al., 2013; Kishi et al., 2003; Li et al., 2020; Novoa et al., 2019; Wang et al., 2019), medaka (Ding et al., 2010; Gopalakrishnan et al., 2013), as well as other annual killifish species (Markofsky and Milstoc, 1979; Walford and Liu, 1965; Wang et al., 2014). However, the lack of genetic and genomic tools for annual killifish, and the relatively long lifespan of other fish models, has limited large-scale exploration of aging and age-related diseases in fish.

Aging represents the primary risk factor for many human pathologies, including cardiovascular and neurodegenerative diseases, cancer, and diabetes (Niccoli and Partridge, 2012). Therefore an exciting approach for treating or postponing the onset of these pathologies, and thus extending human healthspan, is slowing down the aging processes (Lopez-Otin et al., 2013). Traditionally, the study of aging has been primarily conducted in nonvertebrate model organisms, particularly yeast (*Saccharomyces cerevisiae*), worm (*Caenorhabditis elegans*), and fly (*Drosophila melanogaster*), which are naturally short-lived and are magnificent genetic models (Lopez-Otin et al., 2013). Using these models, seminal aging studies have identified evolutionary conserved aging-related pathways, such as the insulin/insulin-like growth factor (IGF) and target of rapamycin pathways (Kenyon, 2010). However, as nonvertebrates, these models lack vertebrate-specific organs and systems (e.g., blood, bones, and an adaptive immune system), as well as many key genes, which are involved in human aging and age-related pathologies (e.g., IL8 and APOE) (Harel et al., 2015). Although vertebrate model systems, particularly the mouse (*Mus musculus*) and zebrafish (*Danio rerio*), have been utilized for genetic studies of aging and related disease, their relatively long lifespan has significantly limited their use (maximal lifespan of mice and zebrafish is 3−4 and 5 years, respectively (Tacutu et al., 2018)). Thus a new experimental vertebrate model was required for exploring and understanding the principles of vertebrate aging.

As is apparent from comparative aging studies, vertebrates age in a similar manner, just at a different pace (Austad, 2010; Harel and Brunet, 2015; Ram and Conn, 2018; Singh et al., 2019). Similarly, old turquoise killifish exhibit a classical range of aging phenotypes that are seen in humans and other vertebrates (Fig. 11.2A) (Fillit et al., 2010; Ram and Conn, 2018), including decline in fertility (Di Cicco et al., 2011; Harel et al., 2015), in wound healing and regeneration (Wendler et al., 2015), and in mitochondrial (Hartmann et al., 2011) and cognitive functions (Valenzano et al., 2006a). Additional histopathological markers include accumulation of lipofuscin in the liver (Terzibasi et al., 2008), upregulation of glial fibrillary acidic protein (GFAP) in the brain (Tozzini et al., 2012) (a marker of neuroinflammation), and increased incidences of neoplastic lesions (Genade et al., 2005; Terzibasi et al., 2008).

Importantly, the lifespan of the turquoise killifish can be manipulated by conserved interventions such as dietary restriction, temperature, and drug treatments (Baumgart et al., 2016; Terzibasi et al., 2009; Valenzano et al., 2006a, 2006b), as well as by the gut microbiota (Smith et al., 2017). In addition to exploring aging, the turquoise killifish possesses many experimental advantages, including an XY-based sexual determination system (Reichwald et al., 2015; Valenzano et al., 2009), embryonic diapause (Hu et al., 2020; Reichwald et al., 2015), which is common in other annual killifish (Podrabsky and Hand, 1999; Romney et al., 2018), and active migration of blastomeres prior to gastrulation (Dolfi et al., 2019; Naumann and Englert, 2018; Wourms, 1972). Finally, the availability of distinct wild populations and wild-derived laboratory strains with different characteristics (Terzibasi et al., 2008) has allowed for the genetic mapping and evolutionary studies of traits, (including color, sex, and lifespan (Cui et al., 2019; Kirschner et al., 2012; Reichwald et al., 2009, 2015; Valenzano et al., 2009, 2015)), as well as extensive ecological studies (Bartakova et al., 2020; Garcia and Reichard, 2020; Polacik et al., 2017; Vrtilek et al., 2018).

Recent advances in genomics and genome engineering approaches have provided efficient and reliable ways to generate precise edits to the genome of a wide range of organisms. This powerful ability, which has been traditionally reserved for a handful of classical model organisms, is now widely accessible for basic and translational research. Initial steps in developing genome engineering for the turquoise killifish were established by applying Tol2-based transgenesis, which allows for random integration and expression of exogenous genes in a temporal and tissue-specific manner (Allard et al., 2013; Harel et al., 2016; Hartmann and Englert, 2012; Valenzano et al., 2011). More recently, two transformative projects were completed in the killifish model organism: a comprehensive genome engineering platform for high-throughput genome editing using CRISPR (clustered regularly interspaced short palindromic repeats) (Harel et al., 2015, 2016) (Fig. 11.2b), and the completion of the back-to-back turquoise killifish genome projects, which provided important information for experimental and evolutionary studies (Reichwald

et al., 2015; Valenzano et al., 2015). Additionally, the highly inbred GRZ strain (Harel and Brunet, 2015; Kim et al., 2016; Valdesalici and Cellerino, 2003) facilitates reference genome assembly, genome engineering, and provides a point of reference among different laboratories using the turquoise killifish.

The ability to efficiently and precisely edit endogenous genes is essential for any experimental genetic model organism. The CRISPR/Cas9 genome engineering tool has revolutionized the ability to edit the genomes of multiple model and non-model organisms (Cong et al., 2013; Jinek et al., 2012; Mali et al., 2013, and reviewed in Hsu et al., 2014). In brief, the Cas9 nuclease is guided by a short guide RNA (gRNA) molecule to a specific genomic locus. There, this ribonucleoprotein complex will generate a double strand break (DSB), which will then be repaired by the error-prone nonhomologous end joining (NHEJ), or by the more accurate homology-directed repair (HDR) (reviewed in Ran et al., 2013). As NHEJ is imprecise, it frequently introduces base-pair addition or deletions, commonly referred to as indels. These indels facilitate the generation of loss-of-function or "knockout" alleles by causing a frameshift mutation, or by deleting large genomic regions when using gRNAs in tandem. On the other hand, HDR repairs the DSB by using a homologous DNA template, and thus can be used to introduce novel sequences into the genome, also known as a "knock-in" (Doudna and Sontheimer, 2014; Heidenreich and Zhang, 2016).

As already mentioned, this system was recently developed for the killifish model, which allowed for the high-throughput generation of knockout and knock-in alleles in multiple aging and disease genes (Harel et al., 2015, 2016; Harel and Brunet, 2015). Together with the availability of a fully sequenced genome, this platform has transformed killifish into a powerful genetic model system for experimental aging research in the lab (Harel et al., 2015, 2016; Harel and Brunet, 2015). For example, knocking out the protein subunit of telomerase has allowed us to generate the fastest vertebrate model for a human age-associated telomere syndrome (e.g., dyskeratosis congenita). Overall, taking advantage of the turquoise killifish's short generation time allows for the generation of stable lines in as quickly as 2−3 months (Harel et al., 2015, 2016; Harel and Brunet, 2015). Since then, this approach was successfully used for generating additional genetic models, such as for exploring diapause (Hu et al., 2020), regeneration (Wang et al., 2020a), and Parkinson's disease (Matsui et al., 2019). In this chapter we describe up-to-date guidelines to establish a large-scale killifish facility, including housing and water parameters, food, breeding strategies, hatching and rearing of fry, and long-term storage of embryos. We describe in detail updated protocols for efficient genome engineering approaches (including CRISPR/Cas9 and Tol2 strategies), which include reagent selection and synthesis, microinjection, genotyping, and troubleshooting.

Large-scale husbandry (including water systems and water parameters)

In contrast to other laboratory fish species, the African turquoise killifish (similar to other annual killifish) undergoes a compressed lifecycle, including an "explosive" growth period, rapid sexual maturity (Dodzian et al., 2018; Harel et al., 2016; Vrtilek et al., 2018), and high fecundity, which requires specific husbandry adaptations. Several protocols have been developed for killifish housing (Dodzian et al., 2018; Harel et al., 2016; Polacik et al., 2016), and here we provide detailed step-by-step adaptations with the focus on genome engineering, lifespan, and aging studies. Additional husbandry considerations are extensively discussed in Chapter 12. Furthermore, as a vertebrate model organism, care and experimental use of turquoise killifish must be approved by and adhere to relevant institutional ethics guidelines.

Housing and water parameters

For reproducible lifespan experiments, constant housing parameters are very important. The turquoise killifish can be housed in commercially available water recirculating systems with a 12 h light/dark cycle (Harel et al., 2016; Smith et al., 2017). Optimal water temperatures range between 26 and 28°C, neutral pH (7−7.5), and water changes of approximately 10% per day are important to maintain water quality (Dodzian et al., 2018; Harel et al., 2016). It is advised that water will be reconstituted from reverse-osmosis (RO) water, added with commercial marine salt, and sodium bicarbonate for adjusting pH. As commonly used in other aquatic species, the water filtration system should include (1) filtration of large solid particles; (2) a biofilter where ammonia is converted to nitrites and nitrates by bacteria; (3) fine mechanical filtration; and (4) UV sterilization. Ammonia, nitrite, and nitrate levels (see "Materials" section) should be monitored frequently.

As the natural habitat of turquoise killifish is mostly ephemeral pans, this fish is relatively hardy and can tolerate a wide range of water parameters (including a range of temperatures, oxygen levels, pH, and salinity) that naturally occur in its seasonal habitat. Similar to its frequently murky and stagnant habitat, the killifish is comfortable in dimmer lighting (such as subdued ceiling lighting), relatively slow water flow (approximately 5−10 L/h), and higher salinity when compared to freshwater fish (commonly 700−2000 μS). Importantly, dimmer lighting reduces algae growth in water tanks, and higher salinity can inhibit velvet disease caused by a parasitic dinoflagellate *Oodinium*.

Male turquoise killifish are largely territorial; thus it is advised that for optimal growth rate, each tank should house a single male with 1−3 females. Although males that are cohoused can demonstrate aggression (Garcia and Reichard, 2020), if grown together from hatching, aggressive behavior is

repressed in some cases. Fish may be housed in 1, 3 or 10 L tanks, with 1−3 L tanks to be used for individual fish housing in lifespan experiments. Killifish are excellent jumpers, therefore to decrease the possibility of strain contamination, lidded tanks and proper labeling are strongly advised. For detailed information regarding the diagnosis and treatment of common fish killifish diseases see Chapter 12, as well as "Diseases of Zebrafish in Research Facilities" from the Zebrafish International Resource Center: https://zebrafish.org/wiki/health/disease_manual/start.

Food

Feeding strategies are discussed in Chapter 12, and here we will briefly mention recommended approaches for optimal fecundity (which is essential for egg collection and genome engineering) and aging studies. Fecundity is highly dependent on food quality and availability, and according to our protocol, peak fertility is reached at 7−9 weeks of age. To optimally support the accelerated growth and rapid sexual maturity (approximately 3−4 weeks posthatching), food consumption is largely higher when compared to other laboratory fish. Therefore at least two feedings per day with high-quality food should be provided. Recently, several commercially available dry food pellets were successfully tested in killifish (Harel et al., 2016; Žák et al., 2020), paving the way to simpler and more standardized housing. Dry food should be supplemented with live/frozen food such as brine shrimp (*Artemia salina*) or blood worms (Blazek et al., 2013) (note that live and frozen blood worms can harbor potential pathogens, and a trusted source is recommended). Fry subsist on brine shrimp until the age of 2 weeks. A small amount of dry food may be given to 1-week-old fry as training but not as a primary food source.

Breeding strategies for genome engineering, including egg collection and incubation

In optimal conditions, the life cycle (from "egg to egg") of the turquoise killifish is 7−9 weeks. Embryonic development in the turquoise killifish is largely nonsynchronous and requires both aquatic and nonaquatic conditions, thus a more "hands-on" approach is required for breeding when compared to other fish models. Normal development from fertilized egg to hatching usually spans 3−4 weeks; however, developmental dormancy through the alternative diapause trajectory can also take place (such as in lower incubation temperatures or in older females) and can largely be avoided by keeping the eggs at 28°C and by breeding young mating pairs. To stimulate embryos to exit diapause a heat-shock treatment could be used, see "Reagent setup and additional protocols" section. There are two main breeding strategies: breeding for strain maintenance and breeding for microinjection and genetic manipulation (which is time sensitive).

Male killifish could be aggressive; therefore it is advised to select a male that is slightly younger and a similar size to the female. When splitting the fish prior to mating, it is advised to keep them in eye contact, such as by using a divider in a 10 L tank or by placing them in two adjacent regular tanks. For injections, plan for a yield of 100−300 eggs according to the observed fecundity in the colony. Crossing 10−20 females is usually sufficient. Cell division in the fertilized eggs is fairly slow, and two-cell stage is observed after 3−4 h. Therefore mating could be allowed for a longer period of time (4−5 h). Fish can be set up for mating weekly, and as frequently as every 3−4 days (Blazek et al., 2013; Podrabsky, 1999). The first few crosses would be mostly for training and might yield a lower number of eggs. Mating using sand trays is more natural for the turquoise killifish, although breeding tanks could be used after fish have been trained to use them. It is important to wash and autoclave sand before using it for the first time and before it is recycled for subsequent uses.

Breeding and embryo incubation for microinjection and genetic manipulation

1. Split males and females in separate tanks at least 2 days before mating. Preferably, keep them separated until mating.
2. On the morning of injection, set up several breeding groups (one male with two to three females) of sexually mature (∼2-month-old) fish using 3 or 10 L tanks.
3. Place plastic trays (∼10 cm in diameter, 4−6 cm in depth) filled with 2 cm of sand for the fish to lay eggs in for 2−5 h.
4. To separate the eggs from the sand, empty the sand tray into a strainer by partially submerging a strainer in a secondary water container using circular motions to let the sand fall through. Killifish eggs are ∼1.2 mm, therefore use a strainer with 0.6 mm hole size.
5. Collect fertilized eggs (or embryos) using a standard plastic Pasteur pipette with the tip cut off. Keep embryos in a 6 cm Petri dish, which can be kept in Yamamoto's embryo solution (Harel et al., 2016) or autoclaved system water (Dodzian et al., 2018). In our protocol we have used Ringer's solution (RS) supplemented with methylene blue (called methylene blue solution) as the basis for all embryo solution (see "Reagent setup and additional protocols" section). Injections should start within 1−2 h for embryos to be at the single-cell or two-cell stage. See the "Microinjection" section below.
6. For disinfecting embryos postinjection, continue to the "Reagent setup and additional protocols". If high mortality is observed, try disinfecting embryos within 24 h after injection to increase survival (see the "Disinfecting embryos by iodine" and "Reagent setup and additional protocols" sections).

7. After injection, keep embryos in 6 cm Petri dishes with 5 mL of methylene blue solution (see the "Reagent setup and additional protocols" section) at a density of up to 50 embryos per dish, and monitor daily for a week. Remove damaged eggs or unfertilized (stained by methylene blue).
8. Incubate embryos at 28°C to increase synchronous embryonic development in 6 cm plates. Replace weekly with 5 mL of fresh methylene blue solution. Remove dead or unfertilized eggs.
9. Keep embryos in solution for 1−2 weeks until black eyes are visible, and proceed to transferring the embryos to a moist solid substrate.
10. Add moist coconut fiber (washed and autoclaved, see the "Reagent setup and additional protocols" section) to the bottom of the 6 cm Petri dishes, and compress it to a flat surface (approximately 0.5 cm deep) using a clean paper towel. Alternatively, moist filter paper can replace the coconut fiber (Dodzian et al., 2018).
11. Using a Pasteur pipette, transfer developed embryos (with black eyes) from the methylene blue solution to the Petri dish containing coconut fiber. Minimize transfer of liquid to keep the plate humid, but not wet. Close the lid of the Petri dish, seal with parafilm to prevent drying, and keep at 28°C. Retain undeveloped embryos in methylene blue solution and monitor their development for 1−2 weeks until they are ready to be transferred. Otherwise, proceed to heat-shock, see the "Reagent setup and additional protocols" section
12. Keep embryos spread apart, with up to ∼50 embryos per 6 cm plate.

Breeding for maintenance

Similar to their natural habitat, killifish embryos require incubation of ∼2 weeks in aqueous solution and ∼2 weeks on a humid substrate. This period could be extended if fish enter diapause. In breeding for line maintenance, the approaches are largely similar, yet less time sensitive, and thus will be discussed in brief. There have been several protocols for line maintenance (Dodzian et al., 2018; Harel et al., 2016; Polacik et al., 2016), and their advantages are discussed in Chapter 12.

Hatching of injected eggs and rearing of fry

The growth rate of fry is highly dependent on the density in which they are placed. Here, we present the maximal density that allows normal growth of the fish. At lower densities, growth is faster (Dodzian et al., 2018). Different approaches for hatching are discussed in Chapter 12.

1. After 2 weeks, transfer all the developed embryos (with golden eyes) from the coconut fiber, using a cut plastic Pasteur pipette, into cold (4°C) humic acid (Dodzian et al., 2018; Harel et al., 2016); for preparation see the "Reagent setup and additional protocols" section. This could be done in a 0.8 L fish tank filled to approximately 1 cm in depth, and placed on the

bench. Alternatively, hatching can be done in a 28°C incubator (Dodzian et al., 2018).

2. To improve oxygen supply, provide aeration with a standard aquarium air pump connected to a tube with an air stone.
3. A day after, fill the tank with an addition of 1:1 system water (or autoclaved water with equivalent salinity) on top of the humic acid, and feed fry daily with freshly hatched brine shrimp. Repeat for 3–4 days. Be sure to remove the dead artemia that the fry have not eaten. The buildup of ammonia from dead artemia may damage the fry.
4. When embryos are hatched prematurely, the majority could end up as "belly-sliders" (i.e., embryos that have not successfully inflated their gas bladder), and many will die. Therefore retain unhatched embryos in solid substrate, and try to hatch them a week later. An alternative is to put the nonhatched embryo in a new cold humic acid solution after 24 h.
5. At 7 days posthatching, separate fry in groups of up to 10 in 1.8 L tanks using a 400 μm fry screen. Place tanks in the main water system, using a slow drip of water flow for several hours to slowly acclimate the fry.
6. Feed twice per day with brine shrimp until 2 weeks of age.
7. At 2 weeks of age, replace with 850 μm fry screen and split fish up to five in a 3 L tank.
8. Once sexually mature (3–4 weeks posthatching), separate into breeding families. Alternatively, for lifespan assays, individually house fish in a 1.8 L tank.
9. Feed adult fish 2–3 times a day with dry food supplemented with live/frozen food (such as brine shrimp or blood worms).
10. See the following table for a brief summary:

Housing					
Age	0–7 days	7–14 days	14 days-maturity (3–4 weeks)	Mature (>3–4 weeks) breeding	Mature (>3–4 weeks) lifespan
Housing density	<30 in a 0.8 L tank (out of the system)	<10 in a 1.8 L tank	<5 in a 3 L tank	<3 in a 3 L tank	1 in a 1.8 L tank
Tank screen	None	400 μm	850 μm	None	None
Feeding					
Brine shrimp	Exclusively	Mainly	Yes	Supplemental only	Yes
Dry food	None	Small amount for training only	Yes	Primarily	Yes
Feeding frequency	Once a day	Twice a day	2–3 times a day	2–3 times a day	2–3 times a day

Reagent setup and additional protocols

Embryo solution

Yamamoto's embryo solution (Harel et al., 2016) or Ringer's solution could be used to maintain embryos. Here, we describe the procedure for Ringer's solution. Dissolve two RINGER tablets/L (Millipore) in double distilled water (DDW). Methylene blue (100 μL/L) should be added to the Ringer's solution (2.3% wt/vol stock solution) to limit parasitic infection. The solution could be kept at room temperature for 2 weeks protected from light. Alternatively, autoclaved system water with methylene blue could be used.

Coconut fiber preparation

Presoak coconut fiber with distilled water and autoclave. Once cooled, squeeze out water (keeping it moist, but not dripping), and keep in closed containers at room temperature, or at 4°C for later use (use within a few weeks). Alternatively, moist filter paper can replace the coconut fiber (Dodzian et al., 2018).

Humic acid preparation

Dissolve 1 g/L humic acid in RO water added with 1 g/L of marine salt. Alternatively, you may use system water (Dodzian et al., 2018). Mix well and autoclave. Refrigerate at 4°C. This will be good for several weeks if kept refrigerated.

Disinfecting embryos by iodine

There are several commonly used approaches for disinfecting fish eggs, including H_2O_2 (Dodzian et al., 2018), iodine, and NaOCl (Harel et al., 2016). Here, we will describe the povidone-iodine (PVP-I) approach (Chang et al., 2015).

1. Prepare a 10% stock solution of PVP-I in DDW, stir carefully. As PVP-I is light sensitive, keep in a dark place (use within 6 months).
2. Freshly prepare 25 ppm iodine working solution: three drops of the stock solution in 40 mL Ringer's solution. Check once a month with an iodine strip tester (Chang et al., 2015).
3. Transfer embryos into a new 6 cm Petri dish, and wash them with 5−7 mL methylene blue solution (to remove debris and dead eggs).
4. Incubate embryos in 5−7 mL of PVP-I solution for 10 min in the same plate.
5. Wash twice in 5−7 mL methylene blue solution for 5 min in the same plate.
6. Fill the plate with methylene blue solution and incubate at 28°C.

Long-term storage of embryos and cryopreservation of sperm

For long-term storage of embryos (tested for up to a year), fertilized and disinfected eggs can be stored at 17°C to induce diapause II, which occurs

after the completion of somitogenesis and prior to development of visible black eyes. Embryos could be stored either in liquid or solid conditions, though using filter papers allows for better monitoring. Eggs that have developed passed this stage should not be kept long term. Recently, a protocol for cryopreservation and in-vitro fertilization of African turquoise killifish was optimized, providing great promise for long-term storage (Antebi et al., 2020).

Receiving or shipping fertilized eggs

For initiating a colony or for distribution of strains, embryos are usually shipped in 6 or 10 cm Petri dishes with moist coconut fiber. This could be done a few days after collection, as well as when eyes are visible. Petri dishes are then sealed with parafilm and, when weather conditions are not below freezing, can be shipped via regular mail. Upon arrival, it is important to disinfect the embryos (see the "Reagent setup and additional protocols" section), and care for them as described earlier. Hatched fish should be kept separately from the colony (preferably in a quarantined area), and their health should be monitored. If fish are healthy, their disinfected progeny can eventually be moved into the main recirculating system.

Heat-shock protocol

Diapause, an alternative developmental trajectory during killifish embryogenesis, is age and temperature dependent. Accordingly, the proportion of diapaused eggs increases when females are at an older age, or egg incubation is at lower temperatures. In the laboratory, as this can slow down routine maintenance, diapaused eggs could resume normal development using a simple heat-shock protocol.

1. Freshly prepare methylene blue solution as described.
2. Add one to three eggs per 0.2 mL PCR tube, and fill with methylene blue solution. Close tubes properly to avoid desiccation.
3. Use the following program on a standard thermocycler during 2–3 days: 6 h at 28°C, 6 h at 37°C.
4. Transfer eggs to a 6 cm Petri dish filled with 5–7 mL of methylene blue solution and keep the plate at 28°C in a humidified incubator. Monitor eggs daily for a week and remove dead eggs. Continue as described in the "Hatching of injected eggs and rearing of fry" section.

Efficient genome engineering approaches

In this section, we will focus on specific adaptations from other fish protocols, tailored specifically for the biology and characteristics of the African turquoise killifish. As commonly used in other fish models, genome engineering approaches have been facilitated by microinjection protocols

(Rembold et al., 2006), transposase systems (Davidson et al., 2003; Grabher and Wittbrodt, 2007; Kawakami et al., 2000) (such as Tol1, Tol2, and Sleeping Beauty), and more recently, genome editing approaches, such as zinc finger nucleases and transcription activator-like effector nucleases (Bedell et al., 2012), and CRISPR/Cas9 (Auer et al., 2014; Chang et al., 2013; Hwang et al., 2013; Jao et al., 2013). Recently, many of these approaches were successfully developed for the turquoise killifish, including CRISPR/Cas9-based genome editing (Harel et al., 2015, 2016), transgenesis (Allard et al., 2013; Harel et al., 2016; Hartmann and Englert, 2012; Valenzano et al., 2011), and microinjection (Harel et al., 2016; Hartmann and Englert, 2012; Valenzano et al., 2011).

In the "Target selection and synthesis of reagents for CRISPR/Cas9 genome editing" section we describe a detailed protocol for CRISPR/Cas9-based genome editing in the turquoise killifish (Harel et al., 2015, 2016), which was recently demonstrated for additional disease models (Matsui et al., 2019), and for exploring diapause (Hu et al., 2020) and regeneration (Wang et al., 2020a). Knock-in alleles via HDR are described elsewhere (Harel et al., 2015, 2016). We include simple guidelines for gRNA target design, microinjection, detection of germline transmission, and minimizing off-target effects. Additionally, in the "Tol2-based transgenesis" section we describe the required adaptations for transgenesis. This step-by-step protocol offers efficient genome engineering for the turquoise killifish, and can be used in small and large killifish colonies alike. The protocol includes three main stages: target selection and synthesis of reagents, injections, and germline transmission.

Target selection and synthesis of reagents for CRISPR/Cas9 genome editing

Target selection can be achieved via CHOPCHOP v2 (Labun et al., 2016), which contains the genome sequence and gene models for the turquoise killifish (Harel et al., 2015; Valenzano et al., 2015). This platform provides detailed parameters and information, predicted efficiency and off-targets, possible restriction sites for confirming successful editing, and oligonucleotide candidates for PCR amplification of the edited region. As demonstrated for other Cas9-based target predictions (Cong et al., 2013; Doudna and Sontheimer, 2014; Jinek et al., 2012; Mali et al., 2013), gRNAs are selected according to the following structure: 5′-(N)20-NGG-3′. The core target sequence is represented by the first 20 base-pairs, while the 3′ "NGG" represents the protospacer adjacent motif site in the genome (Cong et al., 2013; Doudna and Sontheimer, 2014; Jinek et al., 2012; Mali et al., 2013).

Several promoters could be used for the in-vitro transcription (IVT) of gRNA, which might affect the selection of gRNAs. For example, when using the T7 promoter, the first two 5′ nucleotides should be limited to GG (as

described in this protocol), or to GN when using the U6 promoter. It is advised to select two to five different gRNAs for each desired gene of interest, and use the most efficient one for generating the mutation. Next, Cas9 mRNA and the gRNAs are produced by IVT. gRNAs can be synthesized by T7-mediated transcription without the need of cloning. Instead, two annealed oligonucleotides are used as templates (Gagnon et al., 2014; Harel et al., 2015; Hwang et al., 2013), and one of them already contains the T7 promoter sequence. For synthesis of the Cas9 mRNA, SP6-mediated transcription of a codon-optimized nuclear localized version (Jao et al., 2013) (nCas9n) template is available. We have successfully used CRISPR ribonucleoprotein delivery (Harel, unpublished), though we found no added benefit.

Target selection

1. The genome and complete annotation of the turquoise killifish is available through https://www.ncbi.nlm.nih.gov/genome/?term=furzeri. Select a gene (or genes) of interest, and identify conserved regions between vertebrate orthologs using http://genome.ucsc.edu/. These regions are less likely to be alternatively spliced or have an alternative start codon.
2. Identify gRNA target sequences using CHOPCHOP v2 (http://chopchop.cbu.uib.no) (Labun et al., 2016). This platform accepts a range of inputs, including gene identifiers, genomic regions, or pasted sequences. CHOPCHOP ranks the proposed gRNA according to predicted efficiency and number of potential off-targets. Selecting gRNA targets in close proximity to a unique restriction site can facilitate identification of successful editing. Please note that as we are using T7 polymerase for gRNA synthesis, the first two 5′ nucleotides should be limited to Gs, as follows: 5′-GG-(N)18-NGG-3′.
3. Using either CHOPCHOP v2, Primer3 (http://bioinfo.ut.ee/primer3-0.4.0/primer3/), or PrimerBLAST (https://www.ncbi.nlm.nih.gov/tools/primer-blast/index.cgi), select oligonucleotides that are flanking the gRNA sequence, and verify the sequence by Sanger sequencing of the purified PCR product. We recommend 400−700 bp amplicon. Sanger sequencing is advised to verify that naturally occurring genetic variation would not disrupt the selected core gRNA sequence.

gRNA template preparation

1. To generate the template for the gRNA IVT, order standard oligonucleotides (e.g. 200 μM stock concentration) shown in the following table. Additional examples and a comprehensive diagram can be found in Figs. 6 and S4 and Table S1 in Harel et al. (2015) and in Fig. 2A in Harel et al. (2016).

Oligonucleotide	Sequence (5′ to 3′)
Universal reverse oligonucleotide	AAAAGCACCGACTCGGTGCCACTTTTTCAAGTTGATAACGG ACTAGCCTTATTTTAACTTGCTATTTCTAGCTCTAAAAC (used for generation of all gRNA templates)
Variable oligonucleotide	TAATACGACTCACTATA[**GG-(N)18**]GTTTTAGAGCTAGAAATA GCAAG (core target sequence in bold is unique for each gRNA)

Note that as the universal reverse oligonucleotide will be used in all the gRNA template generations, is it advised to aliquot and freeze stocks at −20°C to avoid freeze/thaw cycles.

2. Prepare the following annealing reaction in a PCR tube and mix by pipetting:

Components	Amount (μL)	Final concentration
Universal reverse oligonucleotide (200 μM)	1	20 μM
Variable oligonucleotide (200 μM)	1	20 μM
NEB 2.1 buffer 10X	1	1X
Nuclease-free water	7	
Total	10	

3. Use the following program on a standard thermocycler to anneal the oligonucleotides: 95°C 30 s, 72°C 2 min, 37°C 2 min, 25°C 2 min, 12°C 2 min, 4°C forever. After annealing, 5′ ssDNA overhangs will remain on both sides of the template. Use T4 DNA polymerase to catalyze the gap filling by adding the following to the reaction mix:

Component	Amount (μL)	Final concentration
dNTP mix (25 mM)	0.5	1.25 mM
T4 DNA polymerase (3000 units/mL)	0.5	0.15 units/μL
Nuclease-free water	9	
Total	10	

4. Using a standard thermocycler, incubate the reaction at 12°C for 20 min.
5. Clean the annealed and gap-filled template using a standard PCR purification kit, and elute in 30 μL of Elution Buffer. Expect a concentration of ∼0.5 μg/mL. The template can be stored at −20°C.

Synthesis of gRNAs (1–2 days)

1. For gRNA synthesis, use 1 μL of the eluted template in a 20 μL TranscriptAid T7 High Yield Transcription Kit, according to the manufacturer's instructions (note that scaling down the volume to one-quarter reaction [5 μL] is enough).

2. Following the TURBO DNase treatment (provided in the TranscriptAid T7 kit), precipitate the RNA by adding the following components in the order listed, and mix well before adding the ethanol:

Component	Amount (μL)	Final concentration
Reaction mix	20	
Nuclease-free water	115	
3M Na acetate	15	0.1 mM
GlycoBlue coprecipitant	1	
Ethanol 100% (molecular biology grade)	300	
Total	451	

3. Mix well (or vortex briefly), and chill at −20°C for 15 min to overnight.
4. Pellet the gRNAs for 15 min in a chilled microcentrifuge (4°C) at top speed. Remove the supernatant, briefly respin the tube, and remove residual fluid with a fine-tipped pipet. Note: Do not let the pellet completely dry, otherwise it will not dissolve. Sometimes, due to a high salt content in the kit's buffer, a white ring of pellet will remain after dissolving the RNA; this does not affect the gRNA's effectiveness.
5. Resuspend the pellet in 30 μL dH_2O or 1X TE buffer by letting the tube sit on ice for 30 min. Measure concentration using NanoDrop and adjust for a final concentration of 0.5−1 μg/μL.
6. Run 2 μL of the reaction using a formaldehyde loading dye (provided in the TranscriptAid T7 kit). A discrete band should be seen. Aliquot in 2−3 μL aliquots and store at −80°C.

Synthesis of Cas9 mRNA (1−2 days)

1. Purify the nCas9n expression plasmid DNA (Addgene, #47929 Jao et al., 2013) using a standard Maxiprep Kit.
2. Linearize 5 μg of the nCas9n expression plasmid DNA with 1−2 μL of NotI at 37°C for 2 h. The remaining undigested plasmid significantly reduces mRNA synthesis. Therefore verify complete digestion by gel electrophoresis, and increase incubation time or amount of enzyme if necessary.
3. Purify the digested nCas9n expression plasmid using a PCR purification kit, and elute in 50 μL of 1X Elution Buffer.
4. Transcribe capped and polyadenylated nCas9n mRNA using the mMessage mMachine SP6 kit according to the manufacturer's instructions.
5. Following the TURBO DNase treatment, purify the resulting mRNA using lithium chloride precipitation (provided in the mMessage mMachine SP6 kit). Do not let the pellet fully dry, otherwise it will not dissolve.

6. Resuspend the nCas9n mRNA pellet in dH_2O or TE buffer and incubate at 65°C for 10 min to completely dissolve the mRNA. Adjust to a final concentration of 1−3 μg/μL.
7. Run 2 μL of the reaction using a formaldehyde loading dye (provided in the mMessage mMachine SP6 kit) to test for potential degradation. Prepare 2−3 μL aliquots and store at −80°C.

Tol2-based transgenesis

DNA transposons have been widely used as efficient tools for generating transgenic animals (Clark et al., 2011). The medaka Tol2 element encodes a functional transposase that can facilitate transposition of a DNA construct flanked by specific Tol2 DNA sequences (Kawakami, 2007). This way, a gene cassette can be randomly integrated into the host genome. This system has been demonstrated to be highly efficient in many vertebrate model systems and cell lines, including zebrafish, *Xenopus*, chicken, mouse, and human cells (Kawakami, 2007; Kwan et al., 2007).

Importantly, many steps described in the protocol for the "Target selection and synthesis of reagents for CRISPR/Cas9 genome editing" and "Evaluation of editing efficiency (1−2 days)" sections are not required for Tol2-based transgenesis as a result of the following differences: (1) there is no need for gRNA target selection and synthesis; (2) instead of nCas9n mRNA, Tol2 transposase mRNA is synthesized (the overall protocol for Tol2 mRNA synthesis resembles that of nCasn9 synthesis, with specific differences highlighted below); (3) as we are inserting a foreign sequence into the host genome, a plasmid containing a gene cassette flanked by two Tol2 sequences is required and coinjected; and finally (4) the detection of germline transmission is different because integration is random, and in many cases could be facilitated visually by the use of a fluorescent reporter.

1. Purify the PCS2FA plasmid encoding for the Tol2 transposase (Kwan et al., 2007) using a Maxiprep Kit. The PCS2FA plasmid is available from Dr. Kawakami (kokawaka@lab.nig.ac.jp). Additional details, tools, and alternatives can be found on the Tol2Kit website: http://tol2kit.genetics.utah.edu/index.php/Main_Page.
2. Linearize the PCS2FA plasmid, synthesize, and purify the Tol2 transposase mRNA by following the steps described earlier for nCas9n. (NotI restriction enzyme is also used to linearize PCS2FA.)
3. Prepare your desired construct flanked by specific Tol2 DNA sequences (Kwan et al., 2007).

4. Prepare an injection mixture (35 μL recommended volume) as shown in the following table:

Component	Amount (μL)	Final concentration
Tol2 transposase mRNA (300 ng/μL)	1−2	30 ng/μL
DNA plasmid (400 ng/μL) (containing a transgene of choice flanked by Tol2 sites)	1−2	40 ng/μL
Phenol-red (0.5% wt/vol)	2	0.1% wt/vol
Nuclease-free water	Up to 10	
Total	10	

5. Perform injections as described in step 2, and assess germline transmission visually using a fluorescent stereoscope in the F1 (when fluorescent reporters are used), or use a set of oligonucleotides unique for the transgene for genotyping.

When trying a new promoter, it is recommended to use a small surrogate marker on the same plasmid, such as a fluorescent protein under the control of the *cardiac myosin light chain* (*cmlc*) promoter (Harel et al., 2016; Huang et al., 2003) or the *gamma-crystalin* (*γ-cryst*) promoter (Davidson et al., 2003), which is specifically expressed in the lens. Note that the transgene can randomly integrate into several places in the genome, and outcrosses should be conducted until the construct is inherited in a Mendelian manner. Additionally, new transgenic constructs could be generated using the Tol2Kit (Kwan et al., 2007) with the turquoise killifish bacterial artificial chromosome library (Reichwald et al., 2015).

Microinjection

Overall, the components required for the microinjection are similar to protocols developed for other fish (Rembold et al., 2006), but require specific adaptations.

Equipment setup

- **Preparation of injection needles:** As an adaptation to their environment, the turquoise killifish eggs have a thick chorion. Thus needles have a shorter and less flexible tip than the needles used for zebrafish injections. As each needle puller or filament type will have a different setting, it is advised to compare your results with the examples presented in Fig. 5 in Harel et al. (2016). We present the parameters for borosilicate glass needle designs that have been optimized for filamented microcapillaries on a Sutter Instrument P-87 (with a trough filament). Overall, the tip is best cracked/broken by gently rubbing the tip on a Kimwipe, or breaking it on the chorion before injection (using forceps usually results in an

opening that is too big). Pulled needles can be stored (for years) in a closed Petri dish with two strips of modeling clay to hold them. Importantly, for other pullers and filaments, parameters can change. Use these parameters as a starting point, and optimize based on personal experience and similarity to needle shape.

Pressure	Heat	Pull	Velocity	Time
450	43°C	40	40	250

- **Microinjection procedure (1 day)**
  1. For making the injection mold, boil 1.5%–2% agarose in 50 mL of methylene blue solution and pour 15 mL into a 10 cm Petri dish. Plates could be made in advance, sealed with parafilm and stored at 4°C.
  2. While the agarose is still hot, lay a plastic injection mold on the surface (it will float). Once the mold is removed, this will produce six troughs that will hold eggs in position. A 3D-printing design is available in Harel et al. (2016); make sure to use heat-resistant and nontoxic materials.
  3. Collect eggs for microinjection as mentioned in the "Breeding and embryo incubation for microinjection and genetic manipulation" section.
  4. Prepare the injection mixture as shown in the following table, and keep it on ice.
  5. Immediately before injections, backfill the needle with 5 μL injection mixture using fine pipette tips, as routinely used for gel loading, or alternatively, leaving them upside down in the mixture tube, and wait for the mixture to migrate to the top of the needle.
  6. Note that as a result of the thicker chorion and thicker needles, injections might require some practice. To facilitate piercing through the chorion, embryos can be stored at 4°C for 10 min before injection.

Component	Amount (μL)	Final concentration
Purified gRNA (150–300 ng/μL)	2–4	30 ng/μL
nCas9n mRNA (1–3 μg/μL)	2–6	200–300 ng/μL
Phenol-red (0.5% wt/vol)	4	0.1% wt/vol
Nuclease-free water	Up to 20	
Total	20	

1. Using a stereoscope, place the fertilized eggs into the agar troughs, and orient the single cell (or the two cells) upward toward the injection needle.
2. Using the injection apparatus, inject into the cytoplasm of the single- or two-cell stage embryos using the following parameters: 30 psi with 75 ms pulses—approximately 2.5–10 pL of injection mixture, which corresponds to about 10% of the cell's volume.
3. After injection, disinfect the eggs with PVP-I (see the "Reagent setup and additional protocols" section), monitor embryos daily, and remove dead

embryos (opaque and blue in color). Expect about 30%−50% survival of injected embryos, and about 50% chimeric embryos when using efficient gRNAs.

Note: Adjust back pressure so the needle in the liquid medium looks like a "smoking gun," with slight leaking of the red injection solution from the needle tip. Make sure that a small red diffused dot (phenol-red) is seen in the cell after injection. Injection parameters may vary slightly between different needles and injection apparatuses. To adjust the parameters to achieve a reproducible injection volume, inject into mineral oil placed on top of a micrometer slide (see the "Materials" section) and measure the diameter of a droplet. Injection volume can be calculated according to the following formula: $\frac{4}{3}\pi r^3$. Note the difference between the injection volume in zebrafish (usually between 0.5 and 2 nL).

Evaluation of editing efficiency (1−2 days)

In CRISPR injections, genome editing efficiency of individual (or pooled) gRNAs could be estimated using any of the recently developed approaches, such as restriction enzymes (in which a unique restriction site is disrupted upon successful editing, or a novel one is created Harel et al., 2015; Harel et al., 2016), high-resolution melting (Thomas et al., 2014), CRISPR-STAT (Carrington et al., 2015), and others. In cases where the indel is very small (i.e., 1−2 base-pairs), direct sequencing of the amplified genomic region could be used (Harel et al., 2016). Once an optimal gRNA is selected, additional injections should be done to generate F0 chimeric founders. Although the protocol is focused primarily on CRISPR, it could be used for Tol2-based transgenesis with standard fluorescent markers as readout for success.

1. DNA isolation protocol (Samarut et al., 2016) is performed as follows: prepare the extraction buffer, 50 mM NaOH. Prepare the neutralization buffer, 10 mM Tris HCl pH 8. Store solutions at room temperature for up to 1 year.
2. 48−72 h after injection, isolate genomic DNA from individual embryos by adding 20 μL of extraction buffer to a 1.5 mL tube. Note: Remove remaining methylene blue solution with a fine tip.
3. Crush embryos with a cleaned/autoclaved pestle, spin down, and incubate for 10 min at 95°C.
4. Vortex and spin down, and add 2.2 μL of neutralization solution (1:10 vol/vol).
5. Vortex and spin down at max speed for 1 min. Use 1−2 μL for PCR reaction and proceed to identify successful editing using the methodology of your choice.

6. When successful editing is confirmed on the "test set" of embryos, hatch the remaining injected embryos. Efficiency can range between 0% and 100%, and it is advised to continue if the efficiency is above 10%.

Germline transmission and outcrosses

Set mating pairs with sexually mature F0 chimeric founders. By setting them up with mating pairs with wild-type fish, germline transmission can be evaluated using their progeny (fertilized eggs) by either of the methods described earlier. As their germline could be chimeric, multiple types of indels could be present in an individual fish. Once germline transmission has been confirmed for an individual fish, adult F1 progeny from that successful pair should be genotyped by fin clips or from scales. Heterozygous fish at this stage are considered stable lines, and can be outcrossed to wild-type fish for two to three generations to eliminate potential off-target effects generated by the Cas9 nuclease. For efficient gRNA targets, 2−10 founders are usually sufficient to successfully generate a stable CRISPR line. For the less efficient HDR-based knock-in approach (Harel et al., 2015, 2016), 10−30 founders are usually sufficient.

Genotyping of adult fish

1. Prepare a tricaine stock solution (10 mg/mL): add 1 g sodium bicarbonate and 1 g tricaine to 100 mL molecular biology-grade water. Stir thoroughly using a magnetic stirrer. Keep at 4°C. The solution remains good for several weeks if kept refrigerated.

   Note: Apply breathing mask and safety goggles when handling the powdered tricaine.
2. For genotyping, anesthetize adult fish by adding 4−5 mL of tricaine stock solution in 200 mL of system water. After a few minutes, fish will stop moving.
3. Using a plastic spoon, gently place fish on a sponge (moistened with system water), and quickly trim 2−3 mm from the tail fin with a sterile razor blade. Alternatively, remove two to three scales with forceps or a cotton swab (Dodzian et al., 2018), which is less invasive.
4. Place the tissue in 0.2 mL tubes and process as described in the "Evaluation of editing efficiency (1−2 days)" section.
5. Gently put the fish in 1 L of fresh system water at room temperature to recover for 10 min before returning to the system.

Troubleshooting

Problem	Possible reason	Possible solution
Poor nCas9n or Tol2 mRNA synthesis or degraded product	RNA synthesis kit	Consider aliquoting the synthesis buffer, as it is sensitive to repeated freeze/thaw cycles
	Incomplete digestion of the DNA template	As mentioned earlier, remaining undigested plasmid DNA can lead to very long RNA molecules that can significantly reduce the overall efficiency. Alternatively, gel purification after digestion could be attempted.
	RNase contamination	Use RNase-free reagents and RNase decontamination solutions to clean working surface
Low survival or abnormal development of injected embryos	Nucleic acid toxicity	High concentrations of nucleic acids, primarily DNA, are toxic to the cell. According to our experience, 100 ng/μL of DNA and 330 ng/μL of RNA are safe.
	High injection volume	To prevent physical damage to the injected cell, the injection solution must be lower than 1/10th of the cell's volume (approximately 2.5 −10 pL). Possible solutions include: lowering the injection volume; decreasing the diameter of the needle opening; lowering the air pressure; or decreasing the injection pulse of the injector.
Little or no genome editing detected in injected embryos	Inefficient delivery of injection mixture	Centrifuge the injection mixture at 11,000 g in a chilled centrifuge for 5 min to prevent clogging of the needle
	mRNA degradation	nCas9n and Tol2 mRNA may be degraded. Check mRNA integrity by electrophoresis using agarose gel before making the injection solution.
	Accidental injection into the yolk	Although ssRNA can still be delivered into the cell when injected into the yolk, injections into the cell are more efficient. dsDNA cannot be shuttled this way, and has to be injected directly into the cell. If the single cell is not visible, incubate fertilized eggs at 28°C for 10−30 min to help visualize the single cell. Eggs without a visible single cell at this stage are probably unfertilized.

Fish dissection

Here, we describe a protocol for dissecting and isolating adult killifish organs, which can be used for histology, in situ hybridization, immunohistochemistry, RNA extraction, protein analysis, and other downstream molecular techniques (Fig. 11.3). Although similar protocols, such as for zebrafish (Gupta and Mullins, 2010) exist, aside from characterization of specific organs (D'Angelo, 2013), or anatomy of other killifish species (such as *Aphanius* Motamedi et al., 2019), a detailed description of *N. furzeri* has been lacking.

Experimental setup

1. Prepare two ice buckets, one for dissection and one to keep organs and solutions.
2. Prechill 1X phosphate buffered saline (PBS), and prepare two fine-tipped forceps, two curved forceps, one pair of small scissors, a razor, and one holder for scalpel with affixed scalpel blade.
3. Prepare your euthanasia solution by adding 5 mL of tricaine stock solution (see the "Genotyping of adult fish" section, step 1) to 100 mL of system water.

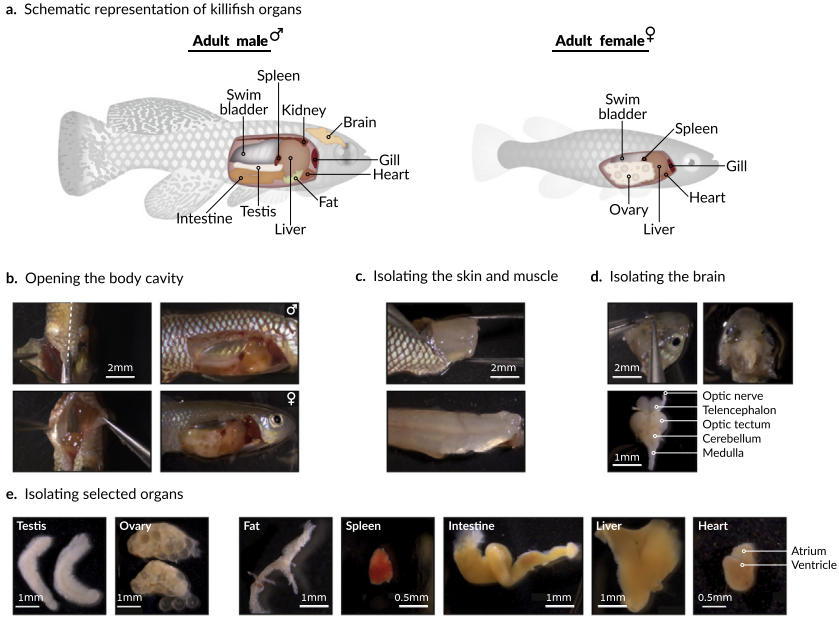

FIGURE 11.3 (A) Adult male and female turquoise killifish *Nothobranchius furzeri* are shown with the anatomical structures labeled. (B–E) A visual protocol for isolating key organs, including opening the body cavity. (B) Organs can be identified according to the anatomical diagram in (A). Isolating the skin and muscle (C), isolating the brain (D), and isolating selected organs, such as the gonads, fat tissue, spleen, intestine, liver, and heart (E).

4. Place fish in the euthanasia solution for 5 min until the operculum stops moving.
5. Using a plastic spoon, place the fish on the operating table.

Organ dissection

At this stage it is possible to bleed the fish by cutting the base of the tail while the heart is still pumping. This will allow a cleaner dissection of the organs with reduced bleeding.

Body cavity dissection

1. Use the scissors to make a cut across the ventral midline of the fish, from the gills to the cloaca. Make shallow and continuous cuts to avoid damaging the internal organs.
2. It is recommended to remove the internal organs from the body cavity to separate the organs more easily. Detach the intestine from the cloaca using scissors or fine-tipped forceps. Hold the detached end of the intestine and pull it outside of the body cavity. Most of the organs will follow.
3. Apply a few drops of 1X PBS on the operation plate and suspend the content of the body cavity. This will allow a better view of the organs, and will be very helpful in younger fish. All the organs removed from the body cavity can be easily separated from one another using scissors or a pair of fine-tipped forceps.
4. The **gastric tract** is readily recognized; it is a long yellowish tube that dominates the body cavity (the color may be affected by the contents of the intestine).
5. The **liver** is the second largest organ within the body cavity; it can be recognized by its size, distinctive color, and shape, which is similar to the mammalian liver.
6. The **gonads** are twin organs located parallel to the intestine. The **testes** are white and elongated, and are comprised of many tubules. The **ovaries** are much larger sacks filled with round eggs at different stages of maturity. The gonads will vary greatly with size as the fish matures.
7. **Adipose tissue can be seen** adjacent to the gonads, and is more visible in old fish. Although it resembles the ovary, it is more transparent and reflective.
8. The **spleen** is a small kidney-shaped dark red-brown organ, and is located near the liver in a loop of the intestine.

Trunk dissection

Detach any remaining organs from the body cavity using scissors and fine-tipped forceps.

1. The **kidneys** are two thin strips of brown tissue that run parallel to the spine ("trunk kidney"), and grow into larger bulbus structures near the head ("head kidney"). Dissect them by locating their posterior tip, and gently use a fine-tipped forceps and scissors to cut across the length of the entire kidney.
2. Detach the **skin** from the **muscle** using forceps. The muscle can be cut using a scalpel, cutting close to the spine to maximize muscle collection.

Dissecting the head

1. The **heart** is located posteriorly and ventrally to the gills. Cut the midline gently through the operculum, and the heart will be at the anterior end of the cut. It is a small, bright red, teardrop shaped, and will most likely still pulse.
2. For isolating the **brain**, use a razor blade to decapitate the head posterior to the gills. Gently remove skin and muscle until you reach the skull; clear the top of the skull.
3. Hold the head from the mouth and lift the skull from the decapitated side using forceps. The skull should come off easily, and the brain will be exposed underneath. Make sure you can see the entirety of the brain, including the **brain stem**, **olfactory bulb**, and **optic nerve**.
4. Cut the optic nerves using scissors and pull the eyes out of their sockets using fine-tipped forceps.
5. Insert a closed fine-tipped forceps underneath the brain and lift it gently. Use either a gentle lifting motion or scissors to detach the brain from the skull. Start at the posterior end, and finish with the olfactory bulb. The brain should come out of the skull in one piece.

Note: Clean working area and surgery equipment between fish with ethanol 70%.

The African turquoise killifish: available toolbox

The African turquoise killifish has been utilized to explore various biological questions, including genomics and genetics, ecology, nutrition and toxicology, embryonic development, regeneration, aging, and more. Here, we will highlight selected studies focusing mostly on "omics" datasets, aging-related phenotypes, recently developed genetic models, and embryonic development.

"Omics" datasets

In recent years, a wide range of studies have generated comprehensive high-throughput datasets exploring killifish biology, as reviewed elsewhere (Cellerino et al., 2015; Harel and Brunet, 2015; Kim et al., 2016; Muck et al.,

2018; Platzer and Englert, 2016). Here, we will highlight a partial list, focusing primarily on aging studies comparing young and old killifish. RNA-seq analyses have been performed by multiple groups to characterize the molecular signature of an aging vertebrate organ, including the skin (Petzold et al., 2013), brain (Baumgart et al., 2014b; Kelmer Sacramento et al., 2020; Petzold et al., 2013), muscle (Cencioni et al., 2019), fin (Baumgart et al., 2016), and a few organs simultaneously (Aramillo Irizar et al., 2018; Baumgart et al., 2017). Other approaches include proteomic analysis of the aging brain using mass spectrometry (Kelmer Sacramento et al., 2020), chromatin landscape of the brain (Harel et al., 2015) and the aging muscle (Cencioni et al., 2019), and sirtuin expression levels in a wide variety of organs (Kabiljo et al., 2019). Among these datasets, it is worth highlighting the killifish genome project (Reichwald et al., 2015; Valenzano et al., 2015), QTL mapping of age-associated traits (Cui et al., 2019; Kirschner et al., 2012; Ng'oma et al., 2014), as well as recent studies exploring vertebrate regeneration (Wang et al., 2020a) and diapause (Hu et al., 2020; Reichwald et al., 2015).

Available genetic models

Transgenesis using Tol2-based random integration was the first step in developing genome engineering approaches in the turquoise killifish (Allard et al., 2013; Harel et al., 2016; Hartmann and Englert, 2012; Valenzano et al., 2011). For example, this technique has allowed tracking of the cell cycle using a FUCCI reporter (Dolfi et al., 2019), a regeneration reporter using the *inhba* enhancer (Wang et al., 2020a), and organ-specific markers, such as the heart (Harel et al., 2016). The ability to manipulate endogenous genes is an essential tool for a genetic model. Indeed, the recent development of CRISPR/Cas9-based efficient genome engineering approaches for the turquoise killifish, including "knockout" and "knock-in" (Harel et al., 2015, 2016), has transformed this organism into a state-of-the-art genetic model. We have characterized a loss-of-function mutation in the gene encoding the protein component of telomerase (TERT) and show that telomerase-deficient turquoise killifish recapitulate characteristics of human pathologies much faster than any other vertebrate model.

Additionally, as a proof of principle for the versatility of this platform, we have recently targeted 13 genes encompassing the hallmarks of aging (generating six stable lines), including cellular senescence and stem cell exhaustion (*p15INK4B*), loss of proteostasis (*ATG5*), deregulated nutrient sensing (*IGF1R, RAPTOR, RPS6KB1*, and *FOXO3*), mitochondrial dysfunction (*POLG*), epigenetic alterations (*ASH2L*), genomic instability (SIRT6), and intercellular communication (*IL8* and *APOE*). We specifically selected genes whose deficiency is expected to slow down (*IGF1R, RAPTOR*, and *RPS6KB1*) or accelerate (*TERT* and *POLG*) the aging process (Lopez-Otin et al., 2013), or have been involved in age-associated diseases, such as *APOE* (Alzheimer's

disease Rhinn et al., 2013), *TERT* (dyskeratosis congenita Armanios, 2009), and *p15INK4B* (cancer Okamoto et al., 1995). Since then, several studies have generated mutant lines, including a loss-of-function mutation in *α-synuclein* to study Parkinson's disease (Matsui et al., 2019), a *CBX7* knockout allele to study the mechanism of diapause (Hu et al., 2020), and the role of a specific enhancer (K-IEN) in regeneration (Wang et al., 2020a).

Neurodegeneration and brain functions

Reflecting its importance in vertebrate aging research, including humans, many killifish studies have explored the age-related decline in behavioral and cognitive functions. These studies identified and characterized a comprehensive range of phenotypes, including a decline in spontaneous exploratory behavior (Smith et al., 2017; Terzibasi et al., 2008; Valenzano et al., 2006a, 2006b; Wei et al., 2020; Yu and Li, 2012), and in learning and memory (tested by both positive and negative conditioning) (Terzibasi et al., 2007, 2008, 2009; Valenzano et al., 2006a, 2006b; Wei et al., 2020; Yu and Li, 2012).

At the cellular level, an increase in age-related neurodegeneration was observed by histological sections and staining with Fluoro Jade B, a pan marker for degenerating neurons (Terzibasi et al., 2007, 2008, 2009; Valenzano et al., 2006b; Wei et al., 2020; Yu and Li, 2012), degeneration of specific types of neurons (Matsui et al., 2019), and inflammatory-associated expression of GFAP (a key component of glia cells) (Matsui et al., 2019; Terzibasi et al., 2009; Tozzini et al., 2012; Wei et al., 2020). Additionally, an age-associated decrease in adult neurogenesis was characterized (Tozzini et al., 2012). Molecular studies have further highlighted the involvement of micro-RNAs (Ripa et al., 2017; Tozzini et al., 2014), CCNB1 (Baumgart et al., 2014a), histone deacetylases (Zupkovitz et al., 2018), NPY and NUCB2B (Montesano et al., 2019a, 2019b), α-synuclein (Matsui et al., 2019), and NGF receptors (de Girolamo et al., 2020).

Cellular aging

Aging is accompanied by changes in cellular composition, as well as a gradual loss of the ability to maintain cellular and physiological homeostasis. In the killifish, several age-dependent signatures, both molecular and histological, have been characterized. For example, lipofuscin, an autofluorescent pigment that accumulates with age in mammals, has been shown to accumulate in killifish tissues with age (Ahuja et al., 2019; Harel et al., 2015, 2016; Liu et al., 2015, 2017b; Terzibasi et al., 2007, 2008, 2009; Tozzini et al., 2013; Valenzano et al., 2006a; Wei et al., 2020; Yu and Li, 2012). Other age-dependent changes include altered cellular composition and accumulation of senescent cells, as detected by senescent-associated beta-galactosidase staining (Genade et al., 2005; Liu et al., 2017b, 2018; Terzibasi et al., 2007; Valenzano et al.,

2006a; Wang et al., 2020b; Wei et al., 2020; Yu and Li, 2012) and an analysis of their unique secretory profile, the senescence-associated secretory phenotype (Liu et al., 2018).

Killifish also display molecular signatures that suggest a decreased ability to maintain cellular homeostasis, as demonstrated by the decline of antioxidant enzymes, the increase in reactive oxidative species, and accumulation of oxidative damage (Blazek et al., 2017; Heid et al., 2017; Liu et al., 2015). Along these same lines, a major cellular component that deteriorates with age in killifish is the mitochondria, with a decrease in mitochondrial numbers, a decrease in the expression of mitogenesis- and OXPHOS-related genes, changes in mitochondrial membrane composition (Almaida-Pagan et al., 2019), as well as a reduction in respiratory chain activity (Baumgart et al., 2016; Hartmann et al., 2011). A decline in proteostasis was recently described, focusing on reduced proteasome activity and overall loss of stoichiometry in protein complexes (Kelmer Sacramento et al., 2020). Finally, telomere attrition is observed, and telomeres shorten with age in the longer-lived MZM lines. Interestingly, as a potential response to telomere attrition, TERT expression increases with age (Hartmann et al., 2009), which may contribute to the observed increased cancer incidences.

Physiological aging

A primary characteristic of the aging process is increased frailty and the decline in organ and physiological functions. Killifish display loss of color with age, reduced muscle mass, known as sarcopenia (Cencioni et al., 2019), and bending of the spine, or kyphosis (Harel and Brunet, 2015; Kim et al., 2016). Metabolic functions are also altered with age, specifically lipid metabolism, including an increase in lipid peroxidation, accumulation of sphingolipids in the heart, and a decrease in cholesterol and triglycerides (Ahuja et al., 2019; Milinkovitch et al., 2018; Wei et al., 2020). Other physiological changes include a decline in fertility and in the quality of eggs leading to slower development of the offspring (before and after hatching) (Api et al., 2018b; Blazek et al., 2013, 2017; Lee et al., 2018; Liu et al., 2017a). Interestingly, even later in life, the offspring of older parents are smaller and less fertile (Api et al., 2018a; Liu et al., 2017a).

Cancer incidence is much higher in older killifish, specifically in the liver and kidneys (Baumgart et al., 2014a; Blazek et al., 2017; Di Cicco et al., 2011; Liu et al., 2017b). Other characteristics include inflammatory signatures (Benayoun et al., 2019; Liu et al., 2017a), and a decline in regenerative capacity of the kidneys, tail, and aberrant wound healing (Benayoun et al., 2019; Hoppe et al., 2015; Hu and Brunet, 2018; Liu et al., 2017a; Wang et al., 2020a; Wendler et al., 2015). Additionally, the diversity of the gut microbiome is reduced with age (Smith et al., 2017). Finally, adaptive immunity, represented by the antibody repertoire, is highly affected with age, demonstrating how the

killifish can become a powerful model for studying adaptative immunosenescence (Bradshaw and Valenzano, 2020).

Diapause

Diapause is an ability to temporarily arrest embryonic development to avoid harsh conditions. There are three developmental stages in which killifish can enter diapause (termed diapause I, II, and III), and the main stage in which diapause primarily happens is diapause II, which occurs during somitogenesis (Api et al., 2018a; Dolfi et al., 2014; Naumann and Englert, 2018). Many of the studies of killifish diapause have been performed on the American species *Austrofundulus limnaeus*, discovering the involvement of protein synthesis, cell cycle arrest, mitochondria, IGF-I, and vitamin D in diapause (Podrabsky and Hand, 1999, 2000; Romney et al., 2018). Recently, several fascinating studies in the turquoise killifish have characterized gene expression signatures during diapause (Hu et al., 2020; Reichwald et al., 2015), observed cell-cycle dynamics of diapause entry and exit, including synchronization of cell division across the embryo body (Dolfi et al., 2014), and involvement of the polycomb complex in long-term preservation of diapause (Hu et al., 2020).

Summary and future perspectives

In recent years, the African turquoise killifish has emerged as a promising experimental model for exploring aging and age-related disease, developmental processes, ecology, and evolution. This expanding interest is supported by a vibrant and growing community worldwide, which meets biennially at the International Nothobranchius Symposium. Following a symposium in Pisa, Jena, and Cologne, the fourth meeting was held in Brno (Czech Republic) as an online meeting in 2021. As an emerging model system, further standardization for husbandry is ongoing, which possibly contributes to the variances in lifespan measurements reported by different labs (Terzibasi et al., 2008; Valdesalici and Cellerino, 2003; Valenzano et al., 2015). Alternatively, it is likely that these differences also reflect natural variability in aging studies, as observed in classical genetic models of aging. Lifespan is a complex multigenic trait, further affected by intricate gene–environment interactions throughout organismal lifespan. As a consequence, lifespan protocols are continuously developed and improved, also for the well-established mouse model (Bellantuono et al., 2020; Bogue et al., 2020). Thus mouse lifespan studies performed in different labs are facing similar challenges as seen in the National Institute on Aging Interventions Testing Program (Nadon et al., 2017).

In this chapter we presented optimized protocols for husbandry and genome engineering, focusing on Tol2-based transgenesis (Allard et al., 2013; Harel et al., 2016; Hartmann and Englert, 2012; Valenzano et al., 2011)

and CRISPR/Cas9-based genome editing (Harel et al., 2015, 2016). This platform should be further expanded to include classical genome editing approaches that allow for conditional gene regulation in-vivo such as Gal4/UAS (Scheer and Campos-Ortega, 1999), Cre/loxP (Dong and Stuart, 2004; Langenau et al., 2005; Pan et al., 2005), and Tet-ON (Huang et al., 2005), as well as the more recent CRISPR interference (Larson et al., 2013; Qi et al., 2013) and CRISPR activation (Dominguez et al., 2016; Gilbert et al., 2014a) (which allow reversible repression or activation of endogenous genes). Genome engineering, particularly CRISPR/Cas9, is a continuously expanding field (Heidenreich and Zhang, 2016; Moon et al., 2019; Smargon et al., 2020; Yeh et al., 2019), which undoubtedly improves existing tools and opens new possibilities. Finally, this protocol could be adapted for genome engineering approaches in other annual and nonannual killifish species, significantly expanding the current state of the art.

Materials

Reagents

- African turquoise killifish (*N. furzeri*) GRZ strain. Available from the authors upon request. CRITICAL: A breeding turquoise killifish colony must be established before attempting this protocol (see the "Reagent setup and additional protocols" section). CAUTION: As a vertebrate model organism, turquoise killifish care and use has to be approved by and must adhere to relevant institutional ethics guidelines. All turquoise killifish care and use in our lab was approved by the Stanford Subcommittee on Research Animal Care.
- Sea salt (Instant Ocean, #SS15-10).
- nCas9n expression plasmid (Jao et al., 2013) (Addgene, #47929).
- Optional: Cas9 protein with NLS (1 mg/mL, PNA Bio). The Cas9 protein can be used instead of nCas9n mRNA.
- Custom DNA oligonucleotides (once annealed will serve as the gRNA template for the in-vitro transcription), 200 μM stock concentration and standard desalted (IDT, Integrated DNA Technologies).
- mMessage mMachine SP6 Ultra Kit (Life Technologies, #AM1340).
- mMessage mMachine T7 Ultra Kit (Life Technologies, #AM1345).
- TranscriptAid T7 High Yield Transcription Kit (Thermo Scientific, #K0441).
- DNase/RNase-free distilled water (Invitrogen, #10977-015).
- 100 bp DNA ladder (Promega, #G2101).
- 1 kb DNA ladder (Promega, #G5711).
- Ethidium bromide (Thermo Scientific, #15585011).
- Agarose (Life Technologies, #16500500).

- UltraPure phenol:chloroform:isoamyl alcohol (25:24:1; Life Technologies, #15593).
- Proteinase K solution (20 mg/mL) (Ambion, #AM2546).
- High Fidelity PCR SuperMix (Invitrogen, #12532-016).
- GoTaq Green Master Mix (Promega, #M712).
- PCR lysis buffer (Viagenbiotech, 102-T).
- Phenol-red solution 0.5% wt/vol (Sigma, #P0290).
- Humic acid (Sigma, #53680). CRITICAL: Humic acid solution needs to be prepared in advance, at least a day before injections. Refrigerate at 4°C. Good for several weeks if kept refrigerated (see the "Reagent setup and additional protocols" section).
- Coconut fiber (ZooMed Item # EE-8, eight dry quarts, loose coconut fiber substrate). CRITICAL: Coconut fiber needs to be prepared in advance, at least a day before it is required (see the "Reagent setup and additional protocols" and "Hatching of injected eggs and rearing of fry" sections).
- Oxygen tablets (Pemble-Halversion, Inc., http://otabs.com/).
- RINGER tablets (Millipore, #1155250001).
- Methylene blue (2.3% wt/vol stock solution, Kordon, #37344).
- Ammonia test kit (API).
- Nitrite test kit (API).
- Nitrate test kit (API).
- NaOH pellets (Sigma, 221465).
- Hydrochloric acid, 36.5%−38.0% (JT Baker, 9535-01).
- Polyvinylpyrrolidone-iodine complex (Acros Organics, 229471000).
- Iodine test strip (Amazon, 2948-BJ).
- TOPO TA Cloning Kit (Life Technologies, #K4600).
- Zero Blunt TOPO PCR Cloning Kit (Life Technologies, #K2800-20).
- One Shot TOP10 Competent *E. Coli* (Life Technologies, #C4040).
- Agarose (Life Technologies, #16500-500).
- EndoFree Maxiprep Kit (Qiagen, #12362).
- NEB buffer 2.1 (NEB #B7202S)T4 DNA polymerase (NEB, #M0203S).
- Deoxynucleotide (dNTP) Solution Set, 100 mM (NEB, #N0446S).
- PCR Purification Kit (Qiagen, #28104).
- GlycoBlue Coprecipitant, 15 mg/mL (Invitrogen, #AM9516).
- Ethylene diamine tetra acetic acid (0.5 M), pH 8.0 (Ambion, #AM9260G).
- Sodium acetate (3 M), pH 5.5 (Ambion, #AM9740).
- QIAquick Nucleotide Removal Kit (Qiagen, #28304).
- Miniprep Kit (Qiagen, #27104).
- NotI (NEB, #R0189S).
- Tricaine (Sigma, #A5040). CAUTION: Tricaine is a hazardous chemical. When handling tricaine powder (or while handling fish that have been exposed to tricaine), protective gloves should be used. Please refer to the Material Safety Data Sheets for more details.
- Potassium chloride (KCl), 2 M (Affymetrix, #75896).

- Otohime Fish Diet (Reed Mariculture).
- Premium Grade Brine Shrimp Eggs (Brine Shrimp Direct).
- Ethanol 100% (200 proof) (Rossville Gold Shield Chemical Co.).
- Isopropanol, ACS plus (Fisher Scientific, #A416-500).
- TE buffer (1X) pH8 (Thermo Fisher, #AM9849).
- Dulbecco's Phosphate Buffered Saline DPBS (Sigma, D8537).

Equipment

- Dumont tweezers #5 (WPI, #500342).
- Gilson PIPETMAN (Fisher Scientific, #F123600G, #F144801G, #F123601G, #F123602G).
- Injection mold (well depth: 1.1 mm; well width: 0.95 mm, see Supplementary Method 1 for 3D-printing design, in STL or DWG file formats, ready to print). CRITICAL: The 3D-printed injection mold should be ordered in advance, depending on the shipping time of locally available providers.
- Phase Lock Gel Tubes Light (Eppendorf 5 Prime, #2302820).
- LB agar plates with 100 μg/mL ampicillin (Teknova, #L1004).
- Borosilicate microcapillaries with filament (Sutter, #BF100-58-10).
- Kimwipe (Kimtech Science).
- Barrier Pipet Tips, Low Binding (Genesee Scientific, #24-401, 24-404, 24-412, 24-430).
- 1.7 mL tubes (Genesee Scientific, #24-282).
- 0.22 μm filter (Genesee Scientific, #25-227).
- Pestle for 1.5 mL tube, RNase and DNase free (Argos, #P7339-901).
- Commercially available water recirculating systems with 2.8 L tanks (Aquaneering, Inc.). CRITICAL: Water recirculating systems are an efficient way to house a breeding turquoise killifish colony, and must be established before attempting this protocol (see the "Reagent setup and additional protocols" section).
- Thermal Cycler (MJ Research PTC-200).
- 60 mm × 15 mm Petri dishes (Fisher, #0875713a).
- Sutter Instrument P-87, Novato, CA.
- Nikon C-PS stereoscope and Zeiss KL 1500 LCD (Stuttgart, Germany) optic fibers.
- Injection apparatus (Applied Scientific Instrumentation, Eugene, OR), which includes an MHC model magnetic stand, an MMPI model pressure injector, a foot switch to pulse the injected solution into the embryos, an MM3 model micromanipulator, and an M-PIP model micropipette holder (Applied Scientific Instrumentation), assisted by a backpressure unit (Warner Instrument, Hamden, CT). CRITICAL: It is recommended that the injection apparatus be assembled according to the manufacturer's guidelines before attempting this protocol.

- 8-Inch Fine Mesh Strainer (OXO Good Grips, #38991).
- Stage micrometer, 1 mm divided into 0.01 mm units (Meiji Techno America, #MA285).
- Compact incubator for embryos (ThermoScientific, #50125590).
- 30 Mesh Sand (Homedepot, #200000278).
- Incubator, 28°C.

Acknowledgements

We thank the Harel lab for stimulating discussion and feedback on the manuscript. We thank Ella Yanay and Ashayma Abu-tair for help with killifish maintenance. Supported by the Zuckerman Program (I.H.), Abisch-Frenkel Foundation 19/HU04 (I.H.), NIH 1R21AG063739 (I.H.), ISF 2178/19 (I.H.), Israel Ministry of Science 3-17631 (I.H.), 3-16872 (I.H.), 3-16591 (E.M), the Moore Foundation GBMF9341 (I.H.), BSF-NSF 2020611 (I.H.), the Israel Ministry of Agriculture 12-16-0010 (I.H), and the Lady Davis Postdoctoral Fellowship (G.A).

References

Ahuja, G., Bartsch, D., Yao, W., Geissen, S., Frank, S., Aguirre, A., Russ, N., Messling, J.E., Dodzian, J., Lagerborg, K.A., et al., 2019. Loss of genomic integrity induced by lysosphingolipid imbalance drives ageing in the heart. EMBO Rep. 20 (4), e47407.

Allard, J.B., Kamei, H., Duan, C., 2013. Inducible transgenic expression in the short-lived fish *Nothobranchius furzeri*. J. Fish. Biol. 82, 1733−1738.

Almaida-Pagan, P.F., Lucas-Sanchez, A., Tocher, D.R., 2014. Changes in mitochondrial membrane composition and oxidative status during rapid growth, maturation and aging in zebrafish, *Danio rerio*. Biochim. Biophys. Acta 1841, 1003−1011.

Almaida-Pagan, P.F., Ortega-Sabater, C., Lucas-Sanchez, A., Gonzalez-Silvera, D., Martinez-Nicolas, A., Rol de Lama, M.A., Mendiola, P., de Costa, J., 2019. Age-related changes in mitochondrial membrane composition of *Nothobranchius furzeri*.: comparison with a longer-living *Nothobranchius* species. Biogerontology 20 (1), 83−92.

Anchelin, M., Alcaraz-Perez, F., Martinez, C.M., Bernabe-Garcia, M., Mulero, V., Cayuela, M.L., 2013. Premature aging in telomerase-deficient zebrafish. Dis. Models Mech. 6, 1101−1112.

Antebi, A., Dolfi, L., Suen, T.K., Ripa, R., 2020. Optimization of cryopreservation and in vitro fertilization techniques for the African turquoise killifish *Nothobranchius furzeri*. bioRxiv. https://doi.org/10.1101/2020.04.14.040824.

Api, M., Biondi, P., Olivotto, I., Terzibasi, E., Cellerino, A., Carnevali, O., 2018a. Effects of parental aging during embryo development and adult life: the case of *Nothobranchius furzeri*. Zebrafish 15, 112−123.

Api, M., Notarstefano, V., Olivotto, I., Cellerino, A., Carnevali, O., 2018b. Breeders age affects reproductive success in *Nothobranchius furzeri*. Zebrafish 15, 546−557.

Aramillo Irizar, P., Schäuble, S., Esser, D., Groth, M., Frahm, C., Priebe, S., Baumgart, M., Hartmann, N., Marthandan, S., Menzel, U., et al., 2018. Transcriptomic alterations during ageing reflect the shift from cancer to degenerative diseases in the elderly. Nat. Commun. 9, 327.

Armanios, M., 2009. Syndromes of telomere shortening. Annu. Rev. Genom. Hum. Genet. 10, 45–61.

Auer, T.O., Duroure, K., De Cian, A., Concordet, J.P., Del Bene, F., 2014. Highly efficient CRISPR/Cas9-mediated knock-in in zebrafish by homology-independent DNA repair. Genome Res. 24, 142–153.

Austad, S.N., 2010. Cats, "rats," and bats: the comparative biology of aging in the 21st century. Integr. Comp. Biol. 50, 783–792.

Bartakova, V., Nagy, B., Polacik, M., Blazek, R., Lamtane, H., Reichard, M., 2020. Genetic diversity of a widespread annual killifish from coastal Tanzania. BMC Evol. Biol. 20, 1.

Baumgart, M., Barth, E., Savino, A., Groth, M., Koch, P., Petzold, A., Arisi, I., Platzer, M., Marz, M., Cellerino, A., 2017. A miRNA catalogue and ncRNA annotation of the short-living fish *Nothobranchius furzeri*. BMC Genomics 18, 693.

Baumgart, M., Di Cicco, E., Rossi, G., Cellerino, A., Tozzini, E.T., 2014a. Comparison of captive lifespan, age-associated liver neoplasias and age-dependent gene expression between two annual fish species: *Nothobranchius furzeri* and *Nothobranchius korthause*. Biogerontology 16 (1), 63–69.

Baumgart, M., Groth, M., Priebe, S., Savino, A., Testa, G., Dix, A., Ripa, R., Spallotta, F., Gaetano, C., Ori, M., et al., 2014b. RNA-seq of the aging brain in the short-lived fish *N. furzeri* - conserved pathways and novel genes associated with neurogenesis. Aging Cell 13 (6), 965–974.

Baumgart, M., Priebe, S., Groth, M., Hartmann, N., Menzel, U., Pandolfini, L., Koch, P., Felder, M., Ristow, M., Englert, C., et al., 2016. Longitudinal RNA-seq analysis of vertebrate aging identifies mitochondrial complex I as a small-molecule-sensitive modifier of lifespan. Cell Syst. 2, 122–132.

Bedell, V.M., Wang, Y., Campbell, J.M., Poshusta, T.L., Starker, C.G., Krug 2nd, R.G., Tan, W., Penheiter, S.G., Ma, A.C., Leung, A.Y., et al., 2012. In vivo genome editing using a high-efficiency TALEN system. Nature 491, 114–118.

Bellantuono, I., de Cabo, R., Ehninger, D., Di Germanio, C., Lawrie, A., Miller, J., Mitchell, S., Navas-Enamorado, I., Potter, P., Tchkonia, T., 2020. A toolbox for the longitudinal assessment of healthspan in aging mice. Nat. Protoc. 15, 540–574.

Benayoun, B.A., Pollina, E.A., Singh, P.P., Mahmoudi, S., Harel, I., Casey, K.M., Dulken, B.W., Kundaje, A., Brunet, A., 2019. Remodeling of epigenome and transcriptome landscapes with aging in mice reveals widespread induction of inflammatory responses. Genome Res. 29, 697–709.

Blazek, R., Polacik, M., Kacer, P., Cellerino, A., Rezucha, R., Methling, C., Tomasek, O., Syslova, K., Terzibasi Tozzini, E., Albrecht, T., et al., 2017. Repeated intraspecific divergence in life span and aging of African annual fishes along an aridity gradient. Evolution 71, 386–402.

Blazek, R., Polacik, M., Reichard, M., 2013. Rapid growth, early maturation and short generation time in African annual fishes. EvoDevo 4, 24.

Bogue, M.A., Philip, V.M., Walton, D.O., Grubb, S.C., Dunn, M.H., Kolishovski, G., Emerson, J., Mukherjee, G., Stearns, T., He, H., 2020. Mouse Phenome Database: a data repository and analysis suite for curated primary mouse phenotype data. Nucleic Acids Res. 48, D716–D723.

Bradshaw, W.J., Valenzano, D.R., 2020. Extreme genomic volatility characterizes the evolution of the immunoglobulin heavy chain locus in cyprinodontiform fishes. Proc. Biol. Sci. 287, 20200489.

Cardona-Costa, J., Perez-Camps, M., Garcia-Ximenez, F., Espinos, F.J., 2009. Effect of gametes aging on their activation and fertilizability in zebrafish (*Danio rerio*). Zebrafish 6, 93–95.

Carney Almroth, B., Johnsson, J.I., Devlin, R., Sturve, J., 2012. Oxidative stress in growth hormone transgenic coho salmon with compressed lifespan–a model for addressing aging. Free Radic. Res. 46, 1183−1189.

Carrington, B., Varshney, G.K., Burgess, S.M., Sood, R., 2015. CRISPR-STAT: an easy and reliable PCR-based method to evaluate target-specific sgRNA activity. Nucleic Acids Res. 43, e157.

Cellerino, A., Valenzano, D.R., Reichard, M., 2015. From the bush to the bench: the annual *Nothobranchius* fishes as a new model system in biology. Biol. Rev. Camb. Phil. Soc. 91 (2), 511−533.

Cencioni, C., Heid, J., Krepelova, A., Rasa, S.M.M., Kuenne, C., Guenther, S., Baumgart, M., Cellerino, A., Neri, F., Spallotta, F., et al., 2019. Aging triggers H3K27 trimethylation hoarding in the chromatin of *Nothobranchius furzeri* skeletal muscle. Cells 8 (10), 1169.

Chang, C.T., Colicino, E.G., DiPaola, E.J., Al-Hasnawi, H.J., Whipps, C.M., 2015. Evaluating the effectiveness of common disinfectants at preventing the propagation of *Mycobacterium* spp. isolated from zebrafish. Comp. Biochem. Physiol. C Toxicol. Pharmacol. 178, 45−50.

Chang, N., Sun, C., Gao, L., Zhu, D., Xu, X., Zhu, X., Xiong, J.W., Xi, J.J., 2013. Genome editing with RNA-guided Cas9 nuclease in zebrafish embryos. Cell Res. 23, 465−472.

Clark, K.J., Urban, M.D., Skuster, K.J., Ekker, S.C., 2011. Transgenic zebrafish using transposable elements. Methods Cell Biol. 104, 137−149.

Cong, L., Ran, F.A., Cox, D., Lin, S., Barretto, R., Habib, N., Hsu, P.D., Wu, X., Jiang, W., Marraffini, L.A., et al., 2013. Multiplex genome engineering using CRISPR/Cas systems. Science 339, 819−823.

Cui, R., Medeiros, T., Willemsen, D., Iasi, L.N.M., Collier, G.E., Graef, M., Reichard, M., Valenzano, D.R., 2019. Relaxed selection limits lifespan by increasing mutation load. Cell 178, 385−399.e320.

D'Angelo, L., 2013. Brain atlas of an emerging teleostean model: *Nothobranchius furzeri*. Anat. Rec. 296, 681−691.

Davidson, A.E., Balciunas, D., Mohn, D., Shaffer, J., Hermanson, S., Sivasubbu, S., Cliff, M.P., Hackett, P.B., Ekker, S.C., 2003. Efficient gene delivery and gene expression in zebrafish using the sleeping beauty transposon. Dev. Biol. 263, 191−202.

de Girolamo, P., Leggieri, A., Palladino, A., Lucini, C., Attanasio, C., D'Angelo, L., 2020. Cholinergic system and NGF receptors: insights from the brain of the short-lived fish *Nothobranchius furzeri*. Brain Sci. 10 (6), 394.

Depczynski, M., Bellwood, D.R., 2005. Shortest recorded vertebrate lifespan found in a coral reef fish. Curr. Biol. 15, R288−R289.

Di Cicco, E., Tozzini, E.T., Rossi, G., Cellerino, A., 2011. The short-lived annual fish *Nothobranchius furzeri* shows a typical teleost aging process reinforced by high incidence of age-dependent neoplasias. Exp. Gerontol. 46, 249−256.

Ding, L., Kuhne, W.W., Hinton, D.E., Song, J., Dynan, W.S., 2010. Quantifiable biomarkers of normal aging in the Japanese medaka fish (*Oryzias latipes*). PLoS One 5, e13287.

Dodzian, J., Kean, S., Seidel, J., Valenzano, D.R., 2018. A protocol for laboratory housing of turquoise killifish (*Nothobranchius furzeri*). J. Vis. Exp. (134), 57073.

Dolfi, L., Ripa, R., Antebi, A., Valenzano, D.R., Cellerino, A., 2019. Cell cycle dynamics during diapause entry and exit in an annual killifish revealed by FUCCI technology. EvoDevo 10, 29.

Dolfi, L., Ripa, R., Cellerino, A., 2014. Transition to annual life history coincides with reduction in cell cycle speed during early cleavage in three independent clades of annual killifish. EvoDevo 5, 32.

Dominguez, A.A., Lim, W.A., Qi, L.S., 2016. Beyond editing: repurposing CRISPR-Cas9 for precision genome regulation and interrogation. Nat. Rev. Mol. Cell Biol. 17, 5−15.

Dong, J., Stuart, G.W., 2004. Transgene manipulation in zebrafish by using recombinases. Methods Cell Biol. 77, 363−379.

Doudna, J.A., Sontheimer, E.J., 2014. The use of CRISPR/Cas9, ZFNs, and TALENs in generating site-specific genome alterations. Preface. Methods Enzymol. 546, xix−xx.

Fillit, H.M., Rockwood, K., Woodhouse, K., 2010. Brocklehurst's Textbook of Geriatric Medicine and Gerontology. Elsevier Health Sciences.

Gagnon, J.A., Valen, E., Thyme, S.B., Huang, P., Ahkmetova, L., Pauli, A., Montague, T.G., Zimmerman, S., Richter, C., Schier, A.F., 2014. Efficient mutagenesis by Cas9 protein-mediated oligonucleotide insertion and large-scale assessment of single-guide RNAs. PLoS One 9, e98186.

Garcia, D., Reichard, M., 2020. The effect of population density on growth and survival of a Neotropical annual killifish. J. Fish. Biol. 97, 298−301.

Genade, T., Benedetti, M., Terzibasi, E., Roncaglia, P., Valenzano, D.R., Cattaneo, A., Cellerino, A., 2005. Annual fishes of the genus *Nothobranchius* as a model system for aging research. Aging Cell 4, 223−233.

Gilbert, L.A., Horlbeck, M.A., Adamson, B., Villalta, J.E., Chen, Y., Whitehead, E.H., Guimaraes, C., Panning, B., Ploegh, H.L., Bassik, M.C., et al., 2014a. Genome-scale CRISPR-mediated control of gene repression and activation. Cell 159, 647−661.

Gilbert, M.J., Zerulla, T.C., Tierney, K.B., 2014b. Zebrafish (*Danio rerio*) as a model for the study of aging and exercise: physical ability and trainability decrease with age. Exp. Gerontol. 50, 106−113.

Gopalakrishnan, S., Cheung, N.K., Yip, B.W., Au, D.W., 2013. Medaka fish exhibits longevity gender gap, a natural drop in estrogen and telomere shortening during aging: a unique model for studying sex-dependent longevity. Front. Zool. 10, 78.

Grabher, C., Wittbrodt, J., 2007. Meganuclease and transposon mediated transgenesis in medaka. Genome Biol. 8 (Suppl. 1), S10.

Gupta, T., Mullins, M.C., 2010. Dissection of organs from the adult zebrafish. J. Vis. Exp. (37), 1717.

Harel, I., Benayoun, B.A., Machado, B., Singh, P.P., Hu, C.K., Pech, M.F., Valenzano, D.R., Zhang, E., Sharp, S.C., Artandi, S.E., et al., 2015. A platform for rapid exploration of aging and diseases in a naturally short-lived vertebrate. Cell 160 (5), 1013−1026.

Harel, I., Brunet, A., 2015. The African turquoise killifish: a model for exploring vertebrate aging and diseases in the fast lane. Cold Spring Harbor Symp. Quant. Biol. 80, 275−279.

Harel, I., Valenzano, D.R., Brunet, A., 2016. Efficient genome engineering approaches for the short-lived African turquoise killifish. Nat. Protoc. 11 (10), 2010−2028.

Hartmann, N., Englert, C., 2012. A microinjection protocol for the generation of transgenic killifish (Species: *Nothobranchius furzeri*). Dev. Dyn. 241, 1133−1141.

Hartmann, N., Reichwald, K., Lechel, A., Graf, M., Kirschner, J., Dorn, A., Terzibasi, E., Wellner, J., Platzer, M., Rudolph, K.L., et al., 2009. Telomeres shorten while Tert expression increases during ageing of the short-lived fish *Nothobranchius furzeri*. Mech. Ageing Dev. 130 (5), 290−296.

Hartmann, N., Reichwald, K., Wittig, I., Drose, S., Schmeisser, S., Luck, C., Hahn, C., Graf, M., Gausmann, U., Terzibasi, E., et al., 2011. Mitochondrial DNA copy number and function decrease with age in the short-lived fish *Nothobranchius furzeri*. Aging Cell 10, 824−831.

Heid, J., Cencioni, C., Ripa, R., Baumgart, M., Atlante, S., Milano, G., Scopece, A., Kuenne, C., Guenther, S., Azzimato, V., et al., 2017. Age-dependent increase of oxidative stress regulates microRNA-29 family preserving cardiac health. Sci. Rep. 7, 16839.

Heidenreich, M., Zhang, F., 2016. Applications of CRISPR-Cas systems in neuroscience. Nat. Rev. Neurosci. 17, 36–44.

Henriques, C.M., Carneiro, M.C., Tenente, I.M., Jacinto, A., Ferreira, M.G., 2013. Telomerase is required for zebrafish lifespan. PLoS Genet. 9, e1003214.

Hoppe, B., Pietsch, S., Franke, M., Engel, S., Groth, M., Platzer, M., Englert, C., 2015. MiR-21 is required for efficient kidney regeneration in fish. BMC Dev. Biol. 15, 43.

Hsu, P.D., Lander, E.S., Zhang, F., 2014. Development and applications of CRISPR-Cas9 for genome engineering. Cell 157, 1262–1278.

Hu, C.K., Brunet, A., 2018. The African turquoise killifish: a research organism to study vertebrate aging and diapause. Aging Cell 17, e12757.

Hu, C.K., Wang, W., Brind'Amour, J., Singh, P.P., Reeves, G.A., Lorincz, M.C., Alvarado, A.S., Brunet, A., 2020. Vertebrate diapause preserves organisms long term through Polycomb complex members. Science 367, 870–874.

Huang, C.J., Jou, T.S., Ho, Y.L., Lee, W.H., Jeng, Y.T., Hsieh, F.J., Tsai, H.J., 2005. Conditional expression of a myocardium-specific transgene in zebrafish transgenic lines. Dev. Dyn. 233, 1294–1303.

Huang, C.J., Tu, C.T., Hsiao, C.D., Hsieh, F.J., Tsai, H.J., 2003. Germ-line transmission of a myocardium-specific GFP transgene reveals critical regulatory elements in the cardiac myosin light chain 2 promoter of zebrafish. Dev. Dyn. 228, 30–40.

Hwang, W.Y., Fu, Y., Reyon, D., Maeder, M.L., Tsai, S.Q., Sander, J.D., Peterson, R.T., Yeh, J.R., Joung, J.K., 2013. Efficient genome editing in zebrafish using a CRISPR-Cas system. Nat. Biotechnol. 31, 227–229.

Jao, L.E., Wente, S.R., Chen, W., 2013. Efficient multiplex biallelic zebrafish genome editing using a CRISPR nuclease system. Proc. Natl. Acad. Sci. U.S.A. 110, 13904–13909.

Jinek, M., Chylinski, K., Fonfara, I., Hauer, M., Doudna, J.A., Charpentier, E., 2012. A programmable dual-RNA-guided DNA endonuclease in adaptive bacterial immunity. Science 337, 816–821.

Kabiljo, J., Murko, C., Pusch, O., Zupkovitz, G., 2019. Spatio-temporal expression profile of sirtuins during aging of the annual fish *Nothobranchius furzeri*. Gene Expr. Patterns 33, 11–19.

Kawakami, K., 2007. Tol2: a versatile gene transfer vector in vertebrates. Genome Biol. 8 (Suppl. 1), S7.

Kawakami, K., Shima, A., Kawakami, N., 2000. Identification of a functional transposase of the Tol2 element, an Ac-like element from the Japanese medaka fish, and its transposition in the zebrafish germ lineage. Proc. Natl. Acad. Sci. U.S.A. 97, 11403–11408.

Kelmer Sacramento, E., Kirkpatrick, J.M., Mazzetto, M., Baumgart, M., Bartolome, A., Di Sanzo, S., Caterino, C., Sanguanini, M., Papaevgeniou, N., Lefaki, M., et al., 2020. Reduced proteasome activity in the aging brain results in ribosome stoichiometry loss and aggregation. Mol. Syst. Biol. 16 (6), e9596.

Kenyon, C., 2010. The genetics of ageing. Nature 464, 504–512.

Kim, Y., Nam, H.G., Valenzano, D.R., 2016. The short-lived African turquoise killifish: an emerging experimental model for ageing. Dis. Models Mech. 9, 115–129.

Kirschner, J., Weber, D., Neuschl, C., Franke, A., Bottger, M., Zielke, L., Powalsky, E., Groth, M., Shagin, D., Petzold, A., et al., 2012. Mapping of quantitative trait loci controlling lifespan in the short-lived fish *Nothobranchius furzeri*–a new vertebrate model for age research. Aging Cell 11, 252–261.

Kishi, S., Uchiyama, J., Baughman, A.M., Goto, T., Lin, M.C., Tsai, S.B., 2003. The zebrafish as a vertebrate model of functional aging and very gradual senescence. Exp. Gerontol. 38, 777–786.

Kwan, K.M., Fujimoto, E., Grabher, C., Mangum, B.D., Hardy, M.E., Campbell, D.S., Parant, J.M., Yost, H.J., Kanki, J.P., Chien, C.B., 2007. The Tol2kit: a multisite gateway-based construction kit for Tol2 transposon transgenesis constructs. Dev. Dyn. 236, 3088−3099.

Labun, K., Montague, T.G., Gagnon, J.A., Thyme, S.B., Valen, E., 2016. CHOPCHOP v2: a web tool for the next generation of CRISPR genome engineering. Nucleic Acids Res. 44, W272−W276.

Langenau, D.M., Feng, H., Berghmans, S., Kanki, J.P., Kutok, J.L., Look, A.T., 2005. Cre/lox-regulated transgenic zebrafish model with conditional myc-induced T cell acute lymphoblastic leukemia. Proc. Natl. Acad. Sci. U.S.A. 102, 6068−6073.

Larson, M.H., Gilbert, L.A., Wang, X., Lim, W.A., Weissman, J.S., Qi, L.S., 2013. CRISPR interference (CRISPRi) for sequence-specific control of gene expression. Nat. Protoc. 8, 2180−2196.

Lee, Y., Drake, A.C., Thomas, N.O., Ferguson, L.G., Chappell, P.E., Shay, K.P., 2018. Dietary resveratrol increases mid-life fecundity of female *Nothobranchius guentheri*. Comp. Biochem. Physiol. C Toxicol. Pharmacol. 208, 71−76.

Li, C., Barton, C., Henke, K., Daane, J., Treaster, S., Caetano-Lopes, J., Tanguay, R.L., Harris, M.P., 2020. celsr1a is essential for tissue homeostasis and onset of aging phenotypes in the zebrafish. eLife 9, e50523.

Liu, S., Zheng, Z., Ji, S., Liu, T., Hou, Y., Li, S., Li, G., 2018. Resveratrol reduces senescence-associated secretory phenotype by SIRT1/NF-κB pathway in gut of the annual fish *Nothobranchius guentheri*. Fish Shellfish Immunol. 80, 473−479.

Liu, T., Liu, S., Ma, L., Li, F., Zheng, Z., Chai, R., Hou, Y., Xie, Y., Li, G., 2017a. Oogenesis, vitellogenin-mediated ovarian degeneration and immune response in the annual fish *Nothobranchius guentheri*. Fish Shellfish Immunol. 66, 86−92.

Liu, T., Ma, L., Zheng, Z., Li, F., Liu, S., Xie, Y., Li, G., 2017b. Resveratrol inhibits age-dependent spontaneous tumorigenesis by SIRT1-mediated post-translational modulations in the annual fish *Nothobranchius guentheri*. Oncotarget 8 (33), 55422−55434.

Liu, T., Qi, H., Ma, L., Liu, Z., Fu, H., Zhu, W., Song, T., Yang, B., Li, G., 2015. Resveratrol attenuates oxidative stress and extends life span in the annual fish *Nothobranchius guentheri*. Rejuvenation Res. 18 (3), 225−233.

Lopez-Otin, C., Blasco, M.A., Partridge, L., Serrano, M., Kroemer, G., 2013. The hallmarks of aging. Cell 153, 1194−1217.

Maldonado, T.A., Jones, R.E., Norris, D.O., 2000. Distribution of beta-amyloid and amyloid precursor protein in the brain of spawning (senescent) salmon: a natural, brain-aging model. Brain Res. 858, 237−251.

Maldonado, T.A., Jones, R.E., Norris, D.O., 2002. Intraneuronal amyloid precursor protein (APP) and appearance of extracellular beta-amyloid peptide (abeta) in the brain of aging kokanee salmon. J. Neurobiol. 53, 11−20.

Mali, P., Yang, L., Esvelt, K.M., Aach, J., Guell, M., DiCarlo, J.E., Norville, J.E., Church, G.M., 2013. RNA-guided human genome engineering via Cas9. Science 339, 823−826.

Markofsky, J., Milstoc, M., 1979. Aging changes in the liver of the male annual cyprinodont fish, *Nothobranchius guentheri*. Exp. Gerontol. 14, 11−20.

Matsui, H., Kenmochi, N., Namikawa, K., 2019. Age- and alpha-synuclein-dependent degeneration of dopamine and noradrenaline neurons in the annual killifish *Nothobranchius furzeri*. Cell Rep. 26, 1727−1733.e1726.

Milinkovitch, T., Lefrancois, C., Durollet, M., Thomas-Guyon, H., 2018. Influence of temperature on age-related lipid peroxidation in a short-lived vertebrate (*Nothobranchius furzeri*). Fish Physiol. Biochem. 44, 343−347.

Montesano, A., Baumgart, M., Avallone, L., Castaldo, L., Lucini, C., Tozzini, E.T., Cellerino, A., D'Angelo, L., de Girolamo, P., 2019a. Age-related central regulation of orexin and NPY in the short-lived African killifish *Nothobranchius furzeri*. J. Comp. Neurol. 527 (9), 1508−1526.

Montesano, A., De Felice, E., Leggieri, A., Palladino, A., Lucini, C., Scocco, P., de Girolamo, P., Baumgart, M., D'Angelo, L., 2019b. Ontogenetic pattern changes of nucleobindin-2/nesfatin-1 in the brain and intestinal bulb of the short lived African turquoise killifish. J. Clin. Med. 9 (1), 103.

Moon, S.B., Ko, J.-H., Kim, Y.-S., 2019. Recent advances in the CRISPR genome editing tool set. Exp. Mol. Med. 51, 1−11.

Motamedi, M., Shamsaldini, F., Teimori, A., Hesni, M.A., 2019. Histomicroscopy and normal anatomy of the adult killifish *Aphanius hormuzensis* (Teleostei; Aphaniidae) from the Persian Gulf coastal environment. Microsc. Res. Tech. 82, 466−480.

Muck, J., Kean, S., Valenzano, D.R., 2018. Chapter 28 - the short-lived African turquoise killifish (*Nothobranchius furzeri*): a new model system for research on aging. In: Ram, J.L., Conn, P.M. (Eds.), Conn's Handbook of Models for Human Aging, second ed. Academic Press, pp. 377−386.

Nadon, N.L., Strong, R., Miller, R.A., Harrison, D.E., 2017. NIA interventions testing program: investigating putative aging intervention agents in a genetically heterogeneous mouse model. EBioMedicine 21, 3−4.

Naumann, B., Englert, C., 2018. Dispersion/reaggregation in early development of annual killifishes: phylogenetic distribution and evolutionary significance of a unique feature. Dev. Biol. 442, 69−79.

Nelson, J.S., Grande, T., Wilson, M.V.H., 2016. Fishes of the World. John Wiley & Sons, Hoboken, New Jersey, p. 1 (online resource).

Ng'oma, E., Reichwald, K., Dorn, A., Wittig, M., Balschun, T., Franke, A., Platzer, M., Cellerino, A., 2014. The age related markers lipofuscin and apoptosis show different genetic architecture by QTL mapping in short-lived *Nothobranchius* fish. Aging (6), 468−480.

Niccoli, T., Partridge, L., 2012. Ageing as a risk factor for disease. Curr. Biol. 22, R741−R752.

Nielsen, J., Hedeholm, R.B., Heinemeier, J., Bushnell, P.G., Christiansen, J.S., Olsen, J., Ramsey, C.B., Brill, R.W., Simon, M., Steffensen, K.F., et al., 2016. Eye lens radiocarbon reveals centuries of longevity in the Greenland shark (*Somniosus microcephalus*). Science 353, 702−704.

Novoa, B., Pereiro, P., Lopez-Munoz, A., Varela, M., Forn-Cuni, G., Anchelin, M., Dios, S., Romero, A., Martinez-Lopez, A., Medina-Gali, R.M., et al., 2019. Rag1 immunodeficiency-induced early aging and senescence in zebrafish are dependent on chronic inflammation and oxidative stress. Aging Cell 18, e13020.

Okamoto, A., Hussain, S.P., Hagiwara, K., Spillare, E.A., Rusin, M.R., Demetrick, D.J., Serrano, M., Hannon, G.J., Shiseki, M., Zariwala, M., et al., 1995. Mutations in the p16INK4/MTS1/CDKN2, p15INK4B/MTS2, and p18 genes in primary and metastatic lung cancer. Cancer Res. 55, 1448−1451.

Pan, X., Wan, H., Chia, W., Tong, Y., Gong, Z., 2005. Demonstration of site-directed recombination in transgenic zebrafish using the Cre/loxP system. Transgenic Res. 14, 217−223.

Petzold, A., Reichwald, K., Groth, M., Taudien, S., Hartmann, N., Priebe, S., Shagin, D., Englert, C., Platzer, M., 2013. The transcript catalogue of the short-lived fish *Nothobranchius furzeri* provides insights into age-dependent changes of mRNA levels. BMC Genomics 14, 185.

Platzer, M., Englert, C., 2016. *Nothobranchius furzeri*: a model for aging research and more. Trends Genet. 32, 543−552.

Podrabsky, J.E., 1999. Husbandry of the annual killifish Austrofundulus limnaeus with special emphasis on the collection and rearing of embryos. Environ. Biol. Fish. 54, 421−431.

Podrabsky, J.E., Hand, S.C., 1999. The bioenergetics of embryonic diapause in an annual killifish, austrofundulus limnaeus. J. Exp. Biol. 202 (Pt 19), 2567–2580.

Podrabsky, J.E., Hand, S.C., 2000. Depression of protein synthesis during diapause in embryos of the annual killifish Austrofundulus limnaeus. Physiol. Biochem. Zool. 73 (6), 799–808.

Polacik, M., Blazek, R., Reichard, M., 2016. Laboratory breeding of the short-lived annual killifish *Nothobranchius furzeri*. Nat. Protoc. 11, 1396–1413.

Polacik, M., Smith, C., Reichard, M., 2017. Maternal source of variability in the embryo development of an annual killifish. J. Evol. Biol. 30, 738–749.

Qi, L.S., Larson, M.H., Gilbert, L.A., Doudna, J.A., Weissman, J.S., Arkin, A.P., Lim, W.A., 2013. Repurposing CRISPR as an RNA-guided platform for sequence-specific control of gene expression. Cell 152, 1173–1183.

Ram, J.L., Conn, P.M., 2018. Conn's Handbook of Models for Human Aging. Academic Press.

Ran, F.A., Hsu, P.D., Wright, J., Agarwala, V., Scott, D.A., Zhang, F., 2013. Genome engineering using the CRISPR-Cas9 system. Nat. Protoc. 8, 2281–2308.

Reichwald, K., Lauber, C., Nanda, I., Kirschner, J., Hartmann, N., Schories, S., Gausmann, U., Taudien, S., Schilhabel, M.B., Szafranski, K., et al., 2009. High tandem repeat content in the genome of the short-lived annual fish *Nothobranchius furzeri*: a new vertebrate model for aging research. Genome Biol. 10, R16.

Reichwald, K., Petzold, A., Koch, P., Downie, B.R., Hartmann, N., Pietsch, S., Baumgart, M., Chalopin, D., Felder, M., Bens, M., et al., 2015. Insights into sex chromosome evolution and aging from the genome of a short-lived fish. Cell 163 (6), 1527–1538.

Rembold, M., Lahiri, K., Foulkes, N.S., Wittbrodt, J., 2006. Transgenesis in fish: efficient selection of transgenic fish by co-injection with a fluorescent reporter construct. Nat. Protoc. 1, 1133–1139.

Rhinn, H., Fujita, R., Qiang, L., Cheng, R., Lee, J.H., Abeliovich, A., 2013. Integrative genomics identifies APOE epsilon4 effectors in Alzheimer's disease. Nature 500, 45–50.

Ripa, R., Dolfi, L., Terrigno, M., Pandolfini, L., Savino, A., Arcucci, V., Groth, M., Terzibasi Tozzini, E., Baumgart, M., Cellerino, A., 2017. MicroRNA miR-29 controls a compensatory response to limit neuronal iron accumulation during adult life and aging. BMC Biol. 15, 9.

Romney, A.L.T., Davis, E.M., Corona, M.M., Wagner, J.T., Podrabsky, J.E., 2018. Temperature-dependent vitamin D signaling regulates developmental trajectory associated with diapause in an annual killifish. Proc. Natl. Acad. Sci. U.S.A. 115, 12763–12768.

Samarut, E., Lissouba, A., Drapeau, P., 2016. A simplified method for identifying early CRISPR-induced indels in zebrafish embryos using High Resolution Melting analysis. BMC Genomics 17, 547.

Scheel, J.J., 1990. Atlas of Killifishes of the Old World (Neptune City, N.J. (1 T.F.H. Plaza, 3rd and Union Aves., Neptune City 07753): T.F.H. Publications.

Scheer, N., Campos-Ortega, J.A., 1999. Use of the Gal4-UAS technique for targeted gene expression in the zebrafish. Mech. Dev. 80, 153–158.

Singh, P.P., Demmitt, B.A., Nath, R.D., Brunet, A., 2019. The genetics of aging: a vertebrate perspective. Cell 177, 200–220.

Smargon, A.A., Shi, Y.J., Yeo, G.W., 2020. RNA-targeting CRISPR systems from metagenomic discovery to transcriptomic engineering. Nat. Cell Biol. 1–8.

Smith, P., Willemsen, D., Popkes, M., Metge, F., Gandiwa, E., Reichard, M., Valenzano, D.R., 2017. Regulation of life span by the gut microbiota in the short-lived African turquoise killifish. eLife 6, e27014.

Tacutu, R., Thornton, D., Johnson, E., Budovsky, A., Barardo, D., Craig, T., Diana, E., Lehmann, G., Toren, D., Wang, J., et al., 2018. Human ageing genomic resources: new and updated databases. Nucleic Acids Res. 46, D1083−D1090.

Terzibasi, E., Lefrançois, C., Domenici, P., Hartmann, N., Graf, M., Cellerino, A., 2009. Effects of dietary restriction on mortality and age-related phenotypes in the short-lived fish *Nothobranchius furzeri*. Aging Cell 8 (2), 88−99.

Terzibasi, E., Valenzano, D.R., Benedetti, M., Roncaglia, P., Cattaneo, A., Domenici, L., Cellerino, A., 2008. Large differences in aging phenotype between strains of the short-lived annual fish *Nothobranchius furzeri*. PLoS One 3, e3866.

Terzibasi, E., Valenzano, D.R., Cellerino, A., 2007. The short-lived fish *Nothobranchius furzeri* as a new model system for aging studies. Exp. Gerontol. 42 (1−2), 81−89.

Thomas, H.R., Percival, S.M., Yoder, B.K., Parant, J.M., 2014. High-throughput genome editing and phenotyping facilitated by high resolution melting curve analysis. PLoS One 9, e114632.

Tozzini, E.T., Baumgart, M., Battistoni, G., Cellerino, A., 2012. Adult neurogenesis in the short-lived teleost *Nothobranchius furzeri*: localization of neurogenic niches, molecular characterization and effects of aging. Aging Cell 11, 241−251.

Tozzini, E.T., Dorn, A., Ng'oma, E., Polacik, M., Blazek, R., Reichwald, K., Petzold, A., Watters, B., Reichard, M., Cellerino, A., 2013. Parallel evolution of senescence in annual fishes in response to extrinsic mortality. BMC Evol. Biol. 13, 77.

Tozzini, E.T., Savino, A., Ripa, R., Battistoni, G., Baumgart, M., Cellerino, A., 2014. Regulation of microRNA expression in the neuronal stem cell niches during aging of the short-lived annual fish *Nothobranchius furzeri*. Front. Cell. Neurosci. 8, 51.

Valdesalici, S., Cellerino, A., 2003. Extremely short lifespan in the annual fish *Nothobranchius furzeri*. Proc. Biol. Sci. 270 (Suppl. 2), S189−S191.

Valenzano, D.R., Benayoun, B.A., Singh, P.P., Zhang, E., Etter, P.D., Hu, C.K., Clément-Ziza, M., Willemsen, D., Cui, R., Harel, I., et al., 2015. The African turquoise killifish genome provides insights into evolution and genetic architecture of lifespan. Cell 163 (6), 1539−1554.

Valenzano, D.R., Kirschner, J., Kamber, R.A., Zhang, E., Weber, D., Cellerino, A., Englert, C., Platzer, M., Reichwald, K., Brunet, A., 2009. Mapping loci associated with tail color and sex determination in the short-lived fish *Nothobranchius furzeri*. Genetics 183, 1385−1395.

Valenzano, D.R., Sharp, S., Brunet, A., 2011. Transposon-mediated transgenesis in the short-lived African killifish *Nothobranchius furzeri*, a vertebrate model for aging. G3 1, 531−538.

Valenzano, D.R., Terzibasi, E., Cattaneo, A., Domenici, L., Cellerino, A., 2006a. Temperature affects longevity and age-related locomotor and cognitive decay in the short-lived fish *Nothobranchius furzeri*. Aging Cell 5, 275−278.

Valenzano, D.R., Terzibasi, E., Genade, T., Cattaneo, A., Domenici, L., Cellerino, A., 2006b. Resveratrol prolongs lifespan and retards the onset of age-related markers in a short-lived vertebrate. Curr. Biol. 16, 296−300.

Vrtilek, M., Zak, J., Polacik, M., Blazek, R., Reichard, M., 2018. Longitudinal demographic study of wild populations of African annual killifish. Sci. Rep. 8, 4774.

Walford, R.L., Liu, R.K., 1965. Husbandry, life span, and growth rate of the annual fish, *Cynolebias adloffi* E. Ahl. Exp. Gerontol. 1, 161−168.

Wang, N., Luo, Z., Jin, M., Sheng, W., Wang, H.T., Long, X., Wu, Y., Hu, P., Xu, H., Zhang, X., 2019. Exploration of age-related mitochondrial dysfunction and the anti-aging effects of resveratrol in zebrafish retina. Aging (Albany NY) 11, 3117−3137.

Wang, W., Hu, C.K., Zeng, A., Alegre, D., Hu, D., Gotting, K., Ortega Granillo, A., Wang, Y., Robb, S., Schnittker, R., et al., 2020a. Changes in regeneration-responsive enhancers shape regenerative capacities in vertebrates. Science (New York, NY) 369 (6508), eaaz3090.

Wang, X., Ren, Y., Du, X., Song, L., Chen, F., Su, F., 2020b. Effects of late-onset dietary intake of salidroside on insulin/insulin-like growth factor-1 (IGF-1) signaling pathway of the annual fish *Nothobranchius guentheri*. Arch. Gerontol. Geriatr. 91, 104233.

Wang, X., Shang, X., Luan, J., Zhang, S., 2014. Identification, expression and function of apolipoprotein E in annual fish *Nothobranchius guentheri*: implication for an aging marker. Biogerontology 15, 233−243.

Wei, J., Qi, H., Liu, K., Zhao, C., Bian, Y., Li, G., 2020. Effects of metformin on life span, cognitive ability, and inflammatory response in a short-lived fish. J Gerontol A Biol Sci Med Sci 75 (11), 2042−2050.

Wendler, S., Hartmann, N., Hoppe, B., Englert, C., 2015. Age-dependent decline in fin regenerative capacity in the short-lived fish *Nothobranchius furzeri*. Aging Cell 14, 857−866.

Wourms, J.P., 1972. The developmental biology of annual fishes. 3. Pre-embryonic and embryonic diapause of variable duration in the eggs of annual fishes. J. Exp. Zool. 182, 389−414.

Yeh, C.D., Richardson, C.D., Corn, J.E., 2019. Advances in genome editing through control of DNA repair pathways. Nat. Cell Biol. 1−11.

Yu, X., Li, G., 2012. Effects of resveratrol on longevity, cognitive ability and aging-related histological markers in the annual fish *Nothobranchius guentheri*. Exp. Gerontol. 47, 940−949.

Žák, J., Dyková, I., Reichard, M., 2020. Good performance of turquoise killifish (*Nothobranchius furzeri*) on pelleted diet as a step towards husbandry standardization. Sci. Rep. 10, 8986.

Zupkovitz, G., Lagger, S., Martin, D., Steiner, M., Hagelkruys, A., Seiser, C., Schöfer, C., Pusch, O., 2018. Histone deacetylase 1 expression is inversely correlated with age in the short-lived fish *Nothobranchius furzeri*. Histochem. Cell Biol. 150 (3), 255−269.